



MINISTRY OF EDUCATION
UNIVERSITY POLITEHNICA OF BUCHAREST

**DOCTORAL SCHOOL OF CHEMICAL ENGINEERING AND
BIOTECHNOLOGIES**



DOCTORAL THESIS

Coordinator:
Prof. Dr. habil Raluca Ioana van Staden

Phd Student:
Oana-Raluca Muşat

Bucharest
2023

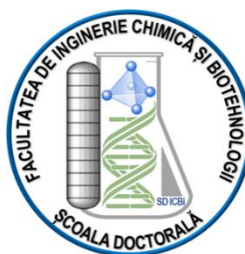


MINISTRY OF EDUCATION

**UNIVERSITY POLITEHNICA OF
BUCHAREST**



**DOCTORAL SCHOOL OF CHEMICAL ENGINEERING AND
BIOTECHNOLOGIES**



DOCTORAL THESIS

**INNOVATIVE METHODS FOR DIAGNOSING
BREAST CANCER**

**Coordinator:
Prof. Dr. habil Raluca Ioana van Staden**

**PhD Student:
Oana-Raluca Muşat**

Bucharest
2023

The doctoral thesis entitled " Innovative Methods for diagnosing" has an extension of 159 pages, includes 7 chapters, presents 33 figures, 2 scheme and 18 tables and cites 374 bibliographic references. The content of the thesis with original numbering of the pages is:

CONTENTS	Thesis page	Summary page
INTRODUCTION	10	8
CHAPTER 1.	13	10
BIOMARKERS USED IN BREAST CANCER DIAGNOSIS	13	10
1.1. Classification of biomarkers used in breast cancer diagnosis and their effects on the individual	13	10
1.1.1. Molecular biomarker for the diagnosis, therapy and prognosis of breast cancer	16	11
1.1.2. Immunohistochemical biomarkers	17	11
1.1.3. Biomarkers involved in diagnosis and therapy	19	12
1.2. Standard classical methods for determining breast cancer biomarkers	19	12
1.2.1. Indicators in early diagnosis of tumour markers	21	13
1.2.2. Standardisations of tumour biomarkers for breast cancer	23	13
1.2.3. Incidence and epidemiology of breast cancer	30	14
1.2.4. Real-time sequencing of a single molecule	31	14
1.2.5. Risk factors leading to tumour development	34	15
1.2.6. Etiopathological, clinic-evolutionary and therapeutic implications breast cancer	35	15
1.3. Tumour markers in breast cancer diagnosis	37	15
1.3.1. The role of breast cancer in the tumor suppressor protein p53.	38	15
1.3.2. Progression and influence of carbohydrate antigen (CA15-3) in breast cancer diagnosis	39	16
CHAPTER 2.	41	17
STOCHASTIC SENSORS USED IN BIOMEDICAL ANALYSIS	41	17
2.1. The sensor, the key element in human analysis	41	17
2.1.1. Smart sensors and mechatronic systems in cell biology	42	17
2.1.2. Biomedical applications and theoretical considerations	43	17

2.2. Apparatus, electrochemical detection and stochastic microsensor design	44	18
2.2.1. Electrochemical detection using stochastic sensors	45	18
2.2.2. Stochastic sensor design	45	19
2.2.3. Stochastic sensor mechanism	46	19
CHAPTER 3.	48	20
D-SERINE AND D-LEUCINE – KEY FACTORS IN BREAST CANCER DIAGNOSIS. ENANTIOANALYSIS OF SERINE AND LEUCINE USING STOCHASTIC SENSORS	48	20
3.1. INTRODUCTION	48	20
3.2. EXPERIMENTAL PART	53	21
3.2.1. Materials and reagents	53	21
3.2.2. Apparatus and reagents	53	22
3.2.3. Design of the enantioselective stochastic sensors	53	22
3.2.4. Stochastic method	55	23
3.2.5. Blood samples	57	25
3.3. RESULTS AND DISCUSSIONS	58	25
3.3.1. Response characteristics of enantioselective stochastic sensors	58	25
3.3.1.1. <i>L- and D-serine</i>	58	25
3.3.1.2. <i>L- and D-leucine</i>	59	27
3.3.2. Selectivity of the proposed sensors used for the determination of serine and leucine	60	28
3.3.2.1. <i>L- and D-serine</i>	60	28
3.3.2.2. <i>L- and D-leucine</i>	61	28
3.3.3. Enantioanalysis of serine in whole blood samples used for the determination of L- and D-serine	62	29
3.3.4. Enantioanalysis of leucine in whole blood samples used for the determination of L- and D-leucine	63	30
3.4. CONCLUSIONS	66	32
CHAPTER 4.	68	33

STOCK MICROSENSORS BASED ON CARBON NANOPULBER FOR ULTRASENSIBLE DETERMINATION OF CA15-3, CEA AND HER-2 IN WHOLE BLOOD	68	33
4.1. INTRODUCTION	68	33
4.2. EXPERIMENTAL PART	70	34
4.2.1. Materials and methods	70	34
4.3. RESULTS AND DISCUSSIONS	72	36
4.3.1. Stochastic sensor response characteristics	72	36
4.3.2. Stability and reproducibility measurements	74	37
4.3.3. Selectivity of stochastic microsensors	74	37
4.3.4. Simultaneous ultrasensitive determination of CA15-3, CEA and HER-2 in whole blood	75	38
4.4. CONCLUSIONS	77	40
CHAPTER 5.	79	41
ULTRASENSIBLE TESTING OF HER-1, HER-2 AND HEREGULIN-α IN WHOLE BLOOD	79	41
5.1. INTRODUCTION	79	41
5.2. EXPERIMENTAL PART	81	42
5.2.1. Materials and reagents	81	42
5.2.2. Apparatus and methods	82	42
5.2.3. Design of the stochastic microsensors	82	42
5.2.4. Recommended procedures: stochastic method	83	42
5.2.5. Samples	85	44
5.3. RESULTS AND DISCUSSIONS	85	44
5.3.1. Morphological characterization and structure of pastes used for stochastic microsensor design	85	44
5.3.2. Response characteristics of the stochastic microsensors	87	45
5.3.3. Stability and reproducibility measurements	89	47
5.3.4. Selectivity	89	47
5.3.5. Ultrasensitive simultaneous determination of HER-1, HER-2 and heregulin-α in whole blood	90	48

5.4. CONCLUSIONS	91	50
CHAPTER 6.	92	51
ULTRASENSITIVE TESTING OF 8-HYDROXY-2'-DEOXYGUANOSINE IN WHOLE BLOOD USING CARBON NANOTUBE-BASED STOCHASTIC MICROSENSORS	92	51
6.1. INTRODUCTION	92	51
6.2. EXPERIMENTAL PART	94	52
6.2.1. Materials, methods and reagents	94	52
6.2.2. Stochastic microsensor design	94	52
6.2.3. Apparatus	94	52
6.2.4. Stochastics method	95	52
6.2.5. Try	96	53
6.3. RESULTS AND DISCUSSIONS	96	53
6.3.1. Morphology of the active surface of the stochastic microsensors	96	53
6.3.2. Ultrasensitive determination of 8-OHdG in whole blood	98	55
6.4. CONCLUSIONS	99	56
CHAPTER 7.	100	57
DETERMINATION OF D-SERINE FROM WHOLE BLOOD SAMPLES USING A ZINC (II)-5-(4-CARBOXYPHENYL)-10,15,20-TRIS (4-PHENOXYPHENYL) PORPHYRIN-BASED ELECTROCHEMICAL SENSOR	100	57
7.1. INTRODUCTION	100	57
7.2. EXPERIMENTAL PART	103	58
7.2.1. Materials and reagents	103	58
7.2.2. Apparatus	103	58
7.2.3. Design of the electrochemical sensor	104	59
7.2.4. Recommended procedure	104	59
7.2.5. Samples	104	59
7.2.6. Selectivity studies	105	59

7.3. RESULTS AND DISCUSSIONS	105	60
7.3.1. Characteristic response of the proposed electrochemical sensor	105	60
7.3.2. Selectivity of the electrochemical sensor	107	61
7.3.3. Determination of D-serine in whole blood samples	108	62
7.4. CONCLUSIONS	110	63
GENERAL CONCLUSIONS	111	64
APPENDIX 1	115	67
APPENDIX 2	116	68
SELECTED REFERENCES	117	69

Objectives of the PhD thesis

This thesis argues innovative methods for cancer diagnosis, analysing electrochemical methods based on stochastic sensors for the identification and analysis of breast cancer type-specific biomarker qualities. The advantages of stochastic sensors were numerous, having a high sensitivity and selectivity, a good correlatio between the results obtained, covering as many linear concentration ranges with detection limits, resulting in a good quality of the sample examined.

INTRODUCTION

Breast cancer has an increased incidence in both males and females. One in nine women develops a breast tumour in her lifetime. In breast cancer, cure is possible when diagnosis is early, in the early stages. Prioritisation and early diagnosis is the key to success in the treatment and success in the treatment and management of breast cancer.

Innovative methods of breast cancer diagnosis have become very important for early and rapid diagnosis of tumours. Screening of patients using classical tests cannot give the necessary information for early diagnosis because of low sensitivity and the limit of determination which is often high than the concentrations of tumour markers in a stage 0 or 1 cancer; also such methods are set for certain biomarkers. Mammograms can provide information, but not at an early stage.

Genetic testing may be indicated if the individual has had a family history (an inheritance of genes or a transmission of mutated genes), suggesting a genetic cause of tumour specific to a particular organ or tissue.

DNA sequencing of the tumour is sometimes performed to determine whether cancer cells present in people who have already been diagnosed with a tumour may have undergone genetic changes. DNA sequencing is a method of determining the nucleotide sequence of a DNA molecule, allowing the structure of the gene to be determined as well as the type of mutation that has produced a genetic disease. DNA sequencing can be used to determine the individual DNA sequences of genes, groups of genes, whole chromosomes or even genomes. Sequencing determines the order of nucleotides present in DNA and RNA molecules isolated from animals, plants, bacteria or any other life form. The results of genetic testing can indicate: CHEK2 (specific to breast cancers, and colorectal cancer) and BRCA1/2 (specific to breast, ovarian, prostate, pancreatic cancers, as well as melanoma).

Some genetic changes can lead to an unexpected or exaggerated response to prescribed medication, and recognition of variants leads to a personalised treatment approach from individual to individual. Given these risks, there is a need for new screening tools and tests capable of bringing the screening test as close as possible to diagnosis at an early stage of breast cancer by: finding specific breast cancer biomarkers (e.g. amino acids) by simultaneously determining 3-8 biomarkers.

Therefore, in this thesis we proposed a new class of sensors – stochastic sensors, for the identification and analysis of breast cancer specific biomarker qualities. D-serine and D-

leucine were identified only in blood samples from patients diagnosed with breast cancer, being an indication that they can be used as specific biomarkers for this type of cancer. Also, the constructed stochastic sensors could be used for the enantioanalysis of serine, leucine and the simultaneous determination of several of several biomarkers such as: carcinoembryonic antigen (CEA), Human Epidermal Growth Factor Receptor 2 (HER-2), Human Epidermal Growth Factor Receptor 1 (HER-1), Heregulin-Alpha, 8-hydroxyguanosine (8OHdG), carbohydrate antigen 15-3 (CA15-3).

CHAPTER I

BIOMARKERS USED IN BREAST CANCER DIAGNOSIS

1.1. Classification of biomarkers used in breast cancer diagnosis and their effects on the individual

Biomarkers are compounds with different chemical structures and sizes [1,2]. In oncology there are a multitude of applications for biomarkers such as> making differential diagnosis, risk assessment, determining malignancy or benignity of a formation, screening, response to treatment, monitoring progression and recurrence, as well as determining prognosis [3,4]. Biomarkers have proven over time to be an effective “tool”, indicating the stage of breast cancer, which is presented as a very important factor in determining future prognosis. In the use of biomarkers, we most commonly encounter nucleic acids, carbohydrates, small metabolites, proteins, cytokines and circulating tumor cells, which control physiological and pharmacological processes [5].

Every day, internal and external influences such as inflammatory reactions, metabolic processes, environmental toxins and radiation cause thousands of random damages to the genetic material (DNA) of every cell in the human body. When the cell cannot be “repaired”, DNA damage, mutations and the development of cancer could be the consequence of early diagnosis. For the diagnosis and planning of an ideal biomarker should follow certain specifications, high sensitivities are detectable by simple methods in biological samples (tissue, blood, urine, sputum, faeces) [6,7]. The implementation of biomarker testing should be done in a targeted way, collecting data from clinical history, paraclinical history and following the currently existing guidelines [8-12]

Normally, a cell is at risk of transforming into a cancer cell when the cellular p 53 tumor suppressor protein is activated. The p53 protein is targeted using various printer methods which we find high performance liquid chromatography (HPLC), ELISA assay. On a large scale, to date, different methods have been investigated for the determination of CA15-3 carbohydrate antigen, the most commonly used being ELISA.

The HER-2 oncogene located on chromosome 17 encodes the synthesis of a transmembrane protein, part of the tyrosine kinase receptor family. The receptors have

homogeneous and functional structures with epidermal growth factor receptors. HER-1 and HER-2/neu are frequently associated with breast tumours. Growth factors that bind to the HER-2 receptor stimulate cell growth and division. CA15-3 is a transmembrane glycoprotein whose synthesis is encoded by the MUC1 gene [35]. The use of the determination of this major marker is to monitor treatment and disease progression in breast tumour, such as: early detection of tumour recurrence in patients previously treated for stage II and III breast carcinoma without clinical signs of disease activity; increased CA15-2 levels in a patient diagnosed with breast tumour indicate a high probability of metastasis; decreased serum CA15-3 levels are an indicator of therapeutic response while increased levels persist and are associated with progressive disease and inadequate response to therapy. When determining the combination of CA15-3 and CEA the sensitivity of detecting tumour recurrence may increase.

Carcinoembryonic antigen (CEA) is one of the oncofetal antigens produced during life as well as during fetal development, after birth production is suppressed and reaches a very low value in adulthood (in individual smokers below 5 ng mL^{-1} , in non-smokers below 3 mL^{-1}) [46].

1.1.1. Molecular biomarker for the diagnosis, therapy and prognosis of breast cancer

In tumor diagnosis, biomarkers are not particularly useful for early detection of breast cancer, but help in determination, treatment monitoring, prognosis and post-treatment follow-up [64-65]. Determination of receptor levels for the hormone called progesterone as well as estrogen is used for early diagnosis of patients with invasive breast cancer to determine eligibility for hormonal treatment. HER-2 is mandatory for assessing the efficacy of anti-HER-2 therapy (trastuzumab, pertuzumab, ado-trastuzumab emtansin or lapatinib) [66,67].

1.1.2. Immunohistochemical biomarkers

Molecular biomarkers used in therapeutic prognosis in breast cancer are represented by the detection of hormone receptors. Using Human Epidermal Growth Factor Receptor 2 (HER-2), carcinoembryonic antigen (CEA), carbohydrate antigen (CA15-3), as well as BRCA1 and BRCA2 genes and other biomarkers all have the ability to positively influence therapeutic management [71-72].

A different genetic test, called tumor DNA sequencing, is sometimes performed to determine whether cancer cells present in people who have already been diagnosed with a

tumor have undergone genetic changes that may provide a clue in treatment by reducing risk [75].

Sanger sequencing is a DNA sequencing method based on the selective incorporation of di-deoxynucleotides by the DNA polymerase enzyme during in vitro DNA replication. The DNA sequencing method allows the determination of the nucleotide sequencing of a DNA molecule. It allows the structure of the gene to be determined, as well as the type of mutation that produced a genetic disease.

1.1.3. Biomarkeri implicați în diagnosticare și terapie

The involvement of biomarkers has detected molecules considered and validated with specificity in the diagnosis of positive breast cancers, as well as the genetic predisposition to develop cancer with this location or irradiation to nearby organs.

Screening for tumor markers are not sensitive or specific enough. Accurate diagnosis in a symptomatic person with cancer has been detected by differentiation from other conditions with similar symptoms. The excess information provided by marker values should be used with caution because there are situations that may decrease or increase marker levels independently of tumour progression or involution. For disease recurrence, we encounter and use tumor markers, along with monitoring treatment response for relapse detection.

1.2. Standard classical methods for determining breast cancer biomarkers

The 4 major components in the treatment of breast cancer remains surgery being a curative method, while hormone therapy, radiotherapy as well as perioperative and adjuvant chemotherapy, which can improve the impact of resectable breast cancer through extensive lymph node dissection.

Randomized trials have not demonstrated that the use of high-dose hematopoietic stem cell- supported therapy improves survival [87-88]. Approximately 16 months with conventional treatment is the median survival: aromatase inhibitors for estrogen receptor-positive tumors and combination chemotherapy for estrogen receptor-positive tumors and chemotherapy for receptor-negative tumors [89].

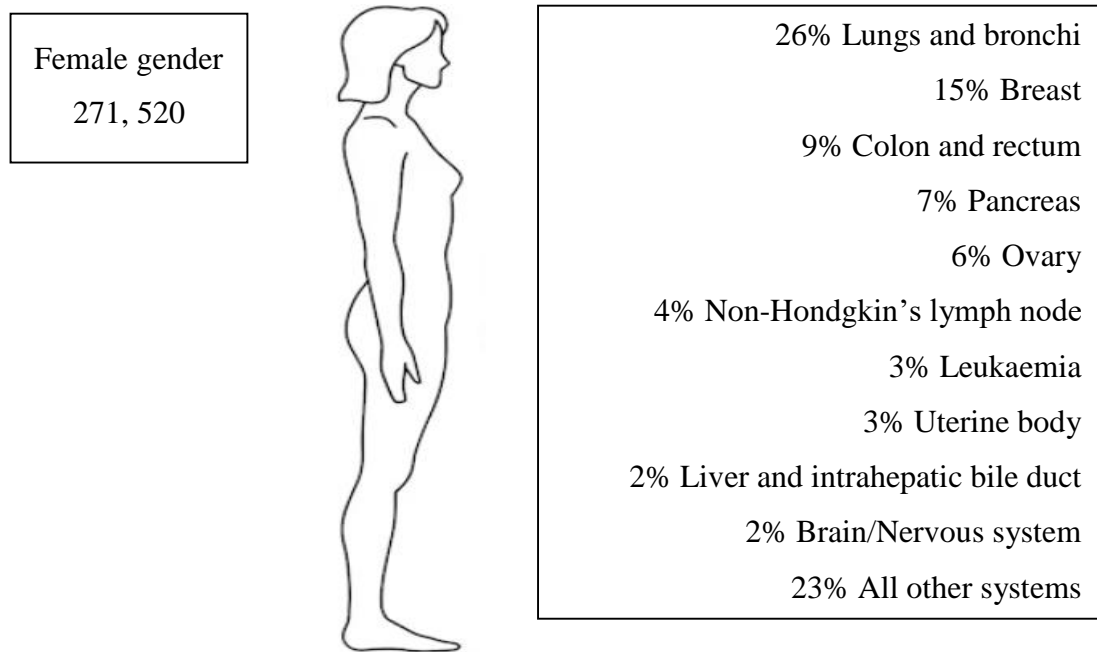


Figure 1.2. Incidence of mammary gland cancer in females compared to the incidence of other cancers².

1.2.1. Standardisations of tumour biomarkers for breast cancer

Breast fibroadenoma is a benign tumour that develops due to the proliferation of connective tissue, which becomes fibrous. This tumour can occur mainly in young women under the age of 30, but can also occur less frequently in women during menopause.

Consequently, tumour markers alone are not a diagnostic criterion for a particular type of cancer, but for certain cancers they provide additional information for an early and accurate prognostic purpose [100].

1.2.2. Standardisations of tumour biomarkers for breast cancer

Tumor markers have been commonly thought of as proteins or other substances produced by both normal and cancer cells, but are produced in greater quantities by cancer cells [101].

They are present in urine, blood, faeces, tumour-specific or other tissues or body fluids from individuals who are suffering from a tumour DNA and tumor gene expression patterns.

Breast tumour staging includes: description of the primary tumour, size and location (ductal/lobular), multicentricity or multifocality, detailing and investigating the type of lymph node invasion (how many nodes are invaded and how many have been investigated, type of

² <http://www.esciencecentral.org/ebooks/cancer-treatment-strategies/cancer-targeting-strategies-revisited.php>

tumour invasion with or without lymphatic node capsule involvement), description of the presence of invasion of blood vessels and lymphatic vessels.

The evaluation includes a complete history, with emphasis on aspects related to the primary tumour, its evolution and menopausal status.

Complete clinical examination, assessment of performance status, haematological, and biochemical evaluation (complete blood count, alkaline phosphatase, liver and kidney function tests) are mandatory. There are two ways of staging: the first is clinical staging, which is based on the outcome of the clinical examination and the information obtained from imaging investigations, and the second staging is pathological staging, which is based on the information obtained from surgery is pathological staging, which is based on the information obtained from surgery and pathological examination of the operative specimen (tumour and lymph nodes) [107, 108].

1.2.3. Incidence and epidemiology of breast cancer

Breastcancer is a malignant proliferation in the epithelial cells that that make up the ducts or lobules of the breast. The frequency of breast cancer is the most common condition found in females. This condition will be characterized by a highly variable course from patient to patient.

The local evolution may last several years, the tumour may be less than 1 cm in diameter, and this interval is very valuable early diagnosis, because the diagnosis of the tumour in the early period, grants maxim chances of cure [112].

1.2.4. Real-time sequencing of a single molecule

Sequencing is used in molecular biology to study genomes and the proteins they encode. The information obtained from sequencing helps researchers discover changes in genes, associations with diseases or phenotypes, and identify targets for new drugs.

DNA is a molecule that provides information about genetic inheritance. DNA sequencing is therefore used in evolutionary biology to study the relatedness of different organisms and how they evolved.

Single-molecule sequencing uses zero-mode waveguide (ZMW) technology [117]. DNA polymerase has a single enzyme that binds to the base zero-mode waveguide, having a single molecule as template. ZMW is a structure that allows the observation of single nucleotide incorporated at a time into the DNA polymerase enzyme. Each of the four bases is attached to a fluorescent waveguide.

Behind nanopore sequencing in theory lies the following: an electric current that can be observed when the nanopore is immersed in a liquid and an electronic potential is applied to it, due to the movement of ions through the nanopore. The amount of current is influenced by the size and shape of the nanopore. When nucleotides pass through the anopore there is a change in the magnitude of the current flowing through that nanopore.

Next-generation sequencing refers to genome sequencing, genome resequencing, transcript sequencing (RNA-Seq), DNA-protein interaction (ChIP sequencing), and epigenome characterization [126]. Resequencing is necessary because the genome of a single individual is not representative of the entire species.

1.2.5. Risk factors leading to tumour development

Risk factors can be divided into personal factors (endogenous) genetic factors and environmental and lifestyle factors (exogenous). The diagnosis of breast cancer is confirmed only by biopsy of the node detected on palpation or evidenced mammographically [131-133].

High risk level of factors are: history of breast cancer, genetic predisposition (BRCA1 and BRCA2 genes are autosomal dominant genes and are involved in most cases of familial cancer), precursor lesions of breast cancer [134-136].

1.2.6. Etiopathological, clinic-evolutionary and therapeutic implications breast cancer

A healthy diet can help prevent this obesity, and the recommendation are: a diet limited in fat intake, increasing consumption of fruits, vegetables, grains, minimizing sugar and salt intake, and most importantly exercising daily for 30 minutes a day can reduce the of diseases such as colon cancer, breast cancer, diabetes and cardiovascular disease [165].

1.3. Tumour markers in breast cancer diagnosis

In breast cancer diagnosis and prognosis, a variety of serum biomarkers representing antigenic determinants such as CEA, CA15-3, Ki67 antigen have been used [179]. Protein levels of these antigens in rerum represent characteristics that indicate risk of tumor development [180,181].

1.3.1. The role of breast cancer in the tumor suppressor protein p53

The tumor suppressor protein in p53 is the most common mutant gene in human cancer. Mutations located in the p17 chromosome are the most common changes, even in human malignancies. In Cancer cells with a mutant p 53, this protein cannot control cell

proliferation for a longer period of time, leading to inefficient DNA repair and genetically unstable cells [185].

1.3.2. Progression and influence of carbohydrate antigen (CA15-3) in breast cancer diagnosis

Carbohydrate antigen is a solid phase enzyme-linked immunosorbent assay (ELISA) based on the sandwich principle for the detection, recurrence verification and diagnosis of tumor marker. CA15-3 is a protein produced by a variety of cells, particularly breast cancer cells.

CHAPTER II

STOCHASTIC SENSORS USED IN BIOMEDICAL ANALYSIS

2.1. The sensor, the key element in human analysis

In approaching stochastic sensors we have found they have many advantages over classical electrochemical sensors in that they are sensitive and selective, having to determine a simultaneous capacity for the compounds of interest, the analysis being carried out in very small quantities of samples analysed, giving high coverage of broad linear concentration ranges with very low detection limits of reliable sample quality analysis.

2.1.1. Smart sensors and mechatronic systems in cell biology

The most commonly used electrochemical sensors in biomedical analysis are amperometric sensors, stochastic sensors and multi-mode sensors [210]. These are based on the observational principle and on changes in current or potential due to interactions occurring at the interface of the sensor with the test sample. Techniques using these sensors are generally classified according to the observing parameter: current (amperometric) potential (potentiometric) or impedance (impedimetric) [211].

2.1.2. Biomedical applications and theoretical considerations

Stochastic analysis is based on the observation of an individual binding event between a single molecule and a receptor. Transmembrane proteins with engineered pores are a promising element in the design of sensors used in stochastic analysis, which in their simple manifestation produce a binary fluent (on/off) response in the transmembrane electric current.

The frequency with the fluctuations occur reveals the concentration of the analyte, and its identity can be inferred from the magnitude or duration of the fluctuations. The frequency of the analyte binding event increases with increasing concentration.

Stochastic detection is a single-molecule detection technique allowing the identification of analytes. The use of these nanopores in the design of stochastic sensors provides an interesting insight into the detection and quantification of single-molecule molecular lithogens Individual interactions between analyte molecules and channel receptor sites can be observed as patterns of current flowing through the channel. Stochastic detection is highly sensitive, the response provided is fast and reversible (allowing real-time analysis of analytes). In addition

to quantitative detection and analyte identification, concurrent detection of multiple analytes is also possible. Stochastic sensors have the highest selectivity [213].

2.2. Apparatus, electrochemical detection and stochastic microsensor design

In stochastic microsensor design, material selection is essential to achieve the desired performance. Stochastic microsensors are based on the working principle of ion channels existing in the human body [214]. The evolution of sensors is related to the two factors: the evolution of material science and pore or channel engineering as well surface analysis techniques. Stochastic microsensors have a membrane that has two basic components: the matrix-material on which the electrochemically active substance is immobilized and the electrochemically active substance that exhibits micro or nanochannels. Molecules with such channels include cyclodextrins, maltodextrins, inulins, antibiotics, crown ethers, biological molecules - which have such channels in their structure, but also molecules that form molecular aggregates and micro/nanochannels, such as porphyrins and phthalocynines. Another classification of substances would be according to origin: biological (e.g. proteins, haemolysin) and synthetic (e.g. cyclodextrins, porphyrins). Directed synthesis of pores of a certain size also facilitates a controlled stochastic sensor response [217].

2.2.1. Electrochemical detection using stochastic sensors

Stochastic sensors are new tools for the rapid detection of tumour markers by an electrochemical method [218,219]. They are integrated into electrochemical cells together with a reference electrode (Ag/AgCl) and a Pt wire (auxiliary electrode) to perform measurements (Figure 2.1).



Figure 2.1. Using the stochastic sensor to screen a blood sample.

2.2.2. Stochastic sensor design

Sensor design is as simple and cost-effective as possible, often using carbon-based materials. A quantity of powdered powder (based on graphite, diamond, nanographene,

graphene, etc.) is mixed with oil on paraffin to obtain a homogeneous paste. A modifier solution (which has the pores required for stochastic analysis) is added to this paste. The modified paste is placed in a tube with an inner diameter of the active surface of 300 μm . A silver wire is inserted into the paste and used to connect the sensor to the external electrical circuit (Figure 2.2). Between measurements, the sensors are rinsed with deionized water to avoid contaminating the samples with each other [221].

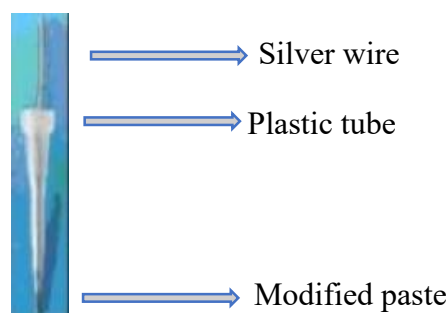


Figure 2.2. – Construction of the stochastic sensor

2.2.3. Stochastic sensor mechanism

The response of stochastic microsensors is based on the channel conductivity when a constant potential is applied. Molecular recognition of the analyte of interest occurs in two steps: initially in step one, the molecular recognition step, the biomarker of interest is extracted from solution at the membrane/solution interface blocking the channel, the current intensity 0 for a certain period of time, called the analyte signature (t_{off}), and in step two the binding step, which takes place when the biomarker interacts with the channel wall. The response of these stochastic sensors is not influenced by matrix composition.

Other advantages over classical methods of analysis are: large working range-allowing determination of biomarkers at different stages of cancer, very low limit of biomarker determination from different biological samples [229-233].

CHAPTER III

D-SERINE AND D-LEUCINE – KEY FACTORS IN BREAST CANCER DIAGNOSIS. ENANTIOANALYSIS OF SERINE AND LEUCINE USING STOCHASTIC SENSORS

3.1. INTRODUCTION

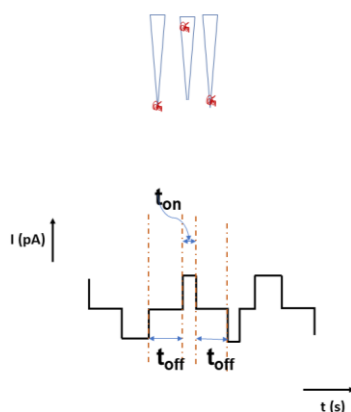
Protonomics and metabolomics play a very important role in cancer research as a valuable source of new biomarkers. Serine levels have been shown to play an important role in breast cancer diagnosis.

Given the importance of biomarkers for rapid and early determination and diagnosis of breast cancer, we proposed serine enantioanalysis as a key factor for early diagnosis of breast cancer. Therefore, a stochastic enantioselective sensor designed by physical immobilisation of Zn(II)-5(4-carboxyphenyl)-10,15,20-tris(4-phenoxyphenyl)-porphyrin in a nanographene paste was used for enantioselective analysis of serine in whole blood samples from healthy volunteers and confirmed breast cancer patients.

The novelty lies in the use of Zn(II)-5(4-carboxyphenyl)-10,15,20-tris(4-phenoxyphenyl) porphyrin as a modifier in the design of an electrochemical sensor, and its use for the enantioanalysis of an amino acid. Its role in the stochastic sensor is to provide the necessary channel for the stochastic response of the sensor.

The main advantages of stochastic sensors when used for biomedical analysis are: no sample preparation is required; matrix complexity does not influence analysis results; multi-analytical analysis is possible.

When the enantiomer signature (t_{off} value) is used, as well as a quantitative analysis using the tonic value measured between two signatures (t_{off} values) (Scheme 3.1.) The principle of current development is based on channel conductivity; in the first stage, the enantiomer enters the channel, blocking it as the current intensity decreases to zero (the enantiomer signature given by the t_{off} value characterizes this stage); inside the channel binding and redox processes take place and equilibrium is reached (the tonic value used for quantitative analysis of enantiomers characterizes this stage).



Scheme 3.1. Current development for stochastic sensors.

The advantages of stochastic sensors over classical electrochemical sensors are: the enantiomer signature does not depend on the matrix composition, but only on the enantiomer size and geometry. The fullerene' N-methyl-fullerene-pyrrolidine derivative was selected because of its ability to provide the necessary channels for stochastic sensing. Fe_2O_3 was added to the graphite paste to improve its conductivity, which facilitated at the selected potential (125mV) signatures and values for t_{on} of the order second magnitude, and therefore the reading was made with high reliability.

The novelty is given by the use of N-methyl-fullerene-pyrrolidine as a modifier of graphite/ Fe_2O_3 and nanographene pastes, for the design of enantioselective stochastic sensors and their use for enantioanalysis of leucine in whole blood samples.

3.2. EXPERIMENTAL PART

3.2.1. Materials and reagents

L-serine, D-serine, paraffin oil, nanographene (particle size less than 3nm, 99.6% carbon content, Zn (II)-5(4-carboxyphenyl)-10,15,20-tris(4-phenoxyphenyl) porphyrin and phosphate buffer were purchased and L- and D-leucine, graphite, Fe_2O_3 graphene nano-pulse, N-methyl-fullerene-pyrrolidine, paraffin oil. Deionized water was used to prepare all solutions. Solutions of L-serine and D-serine (had concentrations ranging from 0,1 mol L⁻¹ to 1fmol L⁻¹) were obtained by serial dilution method; all solutions were treated with phosphate buffer (pH 7.50) and solutions of L- and D-leucine were prepared using phosphate buffer pH 7.40. The concentration range used for both enantiomers was between 1×10^{-20} și 1×10^{-2} mol L⁻¹.

3.2.2. Apparatus and reagents

An Autilab/PGSTAT 12 potentiostat/galvanostat was used for all measurements. Ag/AgCl serving as the reference electrode in the electrochemical cell, while the auxiliary electrode was a Pt wire. The working electrode in the cell was the newly designed enantioselective stochastic sensors.

3.2.3. Design of the enantioselective stochastic sensors

100 μL of 10^{-3} mol L^{-1} mixture of Zn (II)-5(4-carboxyphenyl)-10,15,20-tris(4-phenoxyphenyl)-porphyrin were added to 100 mg of nanographene powder. To this mixture 30 μL of paraffin oil was added to form a modified nanographene paste. The modified paste was analysed using atomic force microscopy (Figure 3.1.). The paste was placed in a special printed tube with a diameter of 300 μm . A silver wire was inserted into the paste and used as an electrical contact. The sensor surface was renewed by polishing with aluminium foil.

Atomic force microscopy experiments were performed using an Agilent Technologies 5500 scanning probe microscope. Images of the modified carbon/diamod layers were acquired in tapping mode (AFM mode AAC) using a silicon cantilever (point probe plus force modulation) with tipp radius < 10 nm (length 227 μm , constant force 1.8 N/m resonance frequency 69 kHz; nanosensors) at scanning speeds from 0.5 to 1 line/s. Images were recorded at 512 x 512 pixel resolution. The imaging and analysis software used was PicoVieq 1.6 (Agilent Technologies, Chandler AZ), with additional image processing (surface profile extraction, filtering, line correction, analytical studies, and 2D and 3D parameters) using Pico Image software.

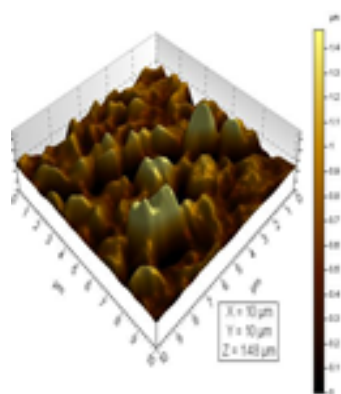


Figure 3.1. AFM 3D image (10X10 mm scan area) of the active surface of the enantioselective stochastic sensor.

For L- and D-leucine, enantioselective stochastic sensor design was performed as follows: 100 mg of graphite/graphene nanopowders were physically mixed with 20 mg of N-methyl-fullerene-pyrrolidine. To the graphite powder mixture, 10 mg of Fe_2O_3 was added. To each of the powders 30 μl of paraffin oil was added to form a homogeneous paste. Each of the

pastes was placed in a non-conductive 3D plastic tube printed in our lab using a 3D printer. The inner diameter of each tube was 25 μm and the length was 1 cm. An Ag wire was used to connect the paste with the external circuit.

The morphology of the designed pastes was investigated using scanning electron microscopy (SEM) (Inspect S, FEI Company, The Netherlands). In order to obtain a good resolution of the microscopic images, the pastes were analysed using the LFD (low vacuum) detector at a high voltage (HV) of 30 kV and magnification of 1600X.

The active surface morphology of the stochastic sensors is shown in Figure 3.2.

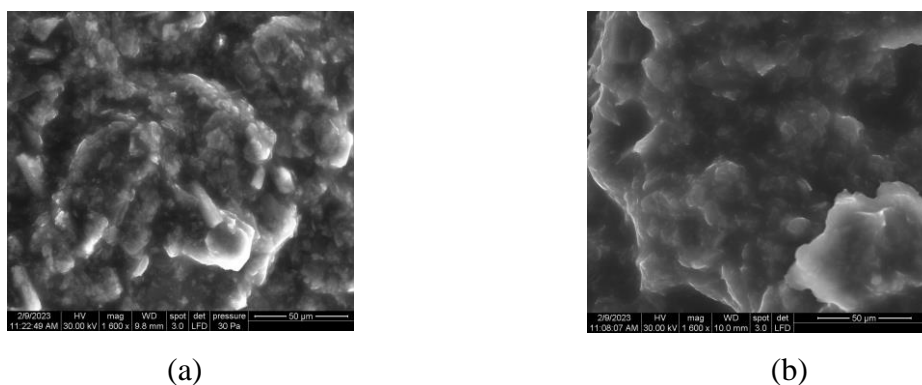


Figure 3.2. SEM images for (a) graphite paste based enantioselective stochastic sensor and (b) nanographene paste based enantioselective stochastic sensor.

3.2.4. Stochastic method

Each series of solutions, respectively L- and D-serine and L- and D-leucine, was analyzed using the proposed stochastic enantioselective sensor at a constant potential of 125mV vs Ag/AgCl, using chronoamperometry as an electrochemical technique. Different signatures (t_{off} values) obtained for each enantiomer were obtained, proving that the sensor is enantioselective. Calibrations were obtained for each enantiomer using the linear regression method. The form of the calibration equation is used, which is: $1/t_{\text{on}}=a+bx\text{Conc}_{\text{enantiomer}}$. The t_{on} value was read between the t_{off} values. The principle of current development is based on channel conductivity: at the entrance to the channel, the enantiomer is blocked and therefore a current decays to zero. The time taken to enter the channel is associated with the signature of the enantiomer (the t_{off} value) and is part of the qualitative analysis. After entering the channel, redox binding processes take place; the sample (Figures 3.3 and 3.4).

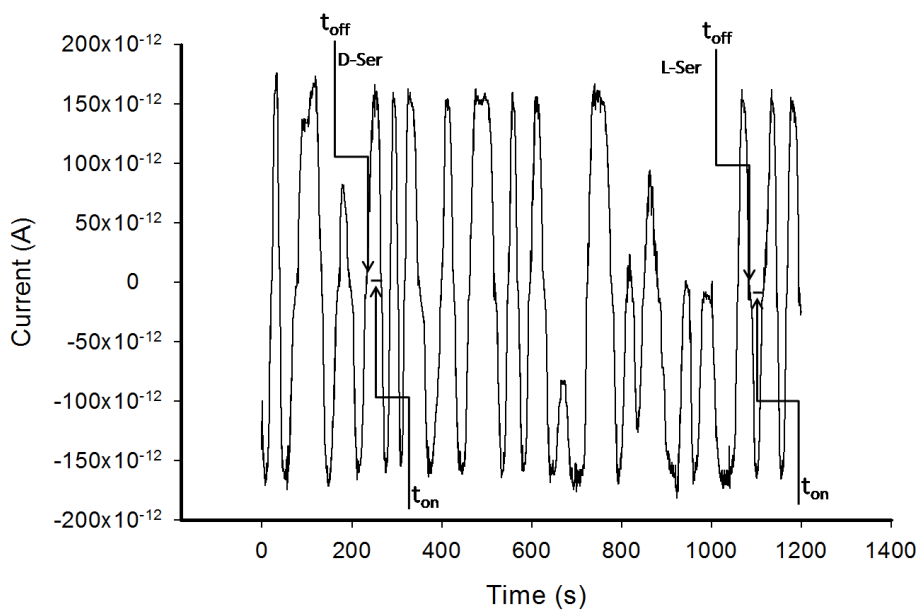
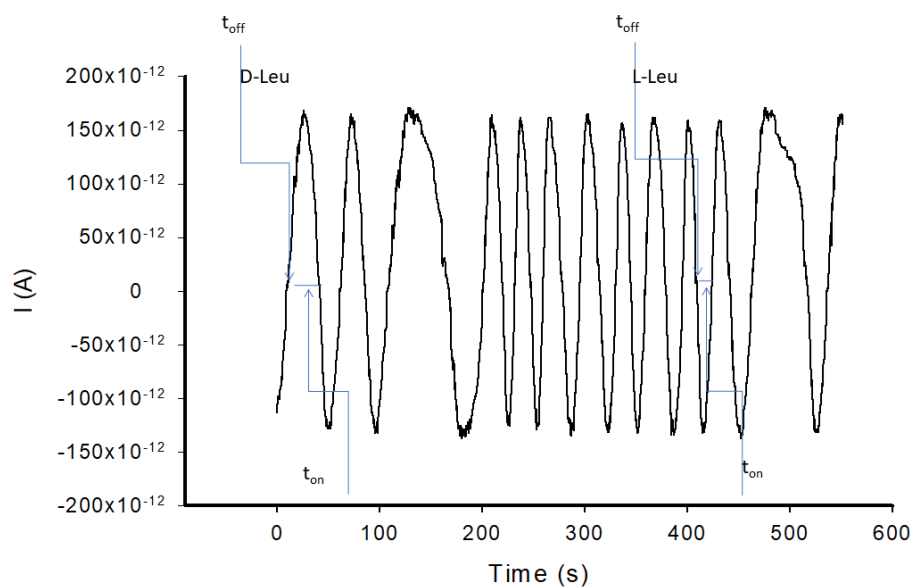
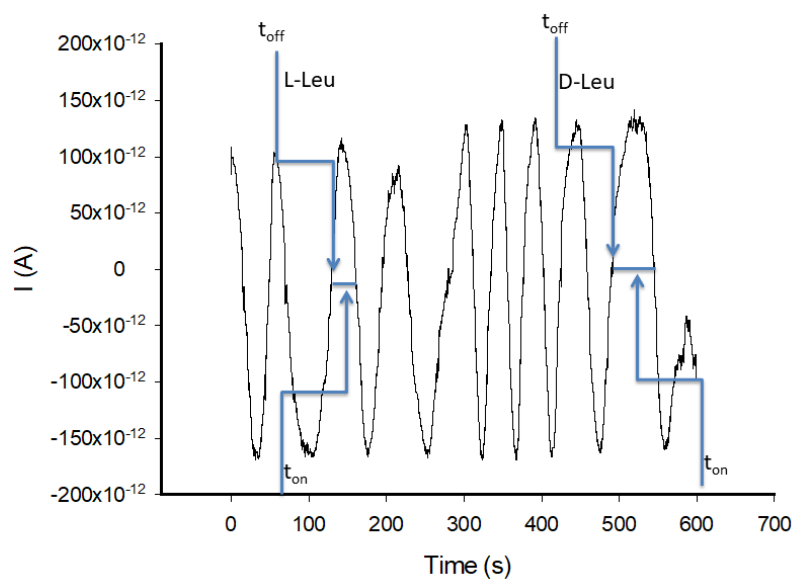


Figure 3.3 . Example of a plot obtained using the stochastic enantioselective sensor (Zn(II)-5(4-carboxyphenyl)-10,15,20-tris(4-phenoxyphenyl)-porphyrin/nanographene) for the determination of L- and D-serinei. $E=125\text{mV vsAg/gCl}$, $C_{L\text{-serine}}=6.12\ \mu\text{mol L}^{-1}$; $C_{D\text{-serine}}=5.07\ \mu\text{mol L}^{-1}$.



(a)



(b)

Figure 3.4. Example plots obtained for the detection of whole blood sample using (a) enantioselective stochastic sensor based on graphite paste and (b) enantioselective stochastic sensor based on nanographene paste.

The determination of L- and D-serine și L- și D-leucine concentration was performed using the calibration equation method by entering the t_{on} value into the corresponding equation.

Enzyme-linked immunosorbent assay (ELISA) is a standard method used for the determination of serine enantiomers.

3.2.5. Blood samples

Whole blood samples from healthy volunteers as well as from patients as well as from confirmed breast cancer patients were obtained from the University Hospital Bucharest (Ethics Committee approval no 11/2013; informed consent was obtained from all subjects). Whole blood samples were analyzed without any pretreatment.

3.3. RESULTS AND DISCUSSIONS

3.3.1. Response characteristics of enantioselective stochastic sensors

3.3.1.1. L- and D-serine

All response characteristics were determined by 25°C using chronoamperometry at 125 mV potential temperature versus Ag/AgCl.

First, the signatures (t_{off} values) of L- and D-serine were analyzed and determined. The signature for L-serine was 1.8 s, while the signature for D-serine was 1.0 s.

Table 3.1. Enantioanalyze serine in whole blood obtained from confirmed breast cancer patients using stochastic enantioselective sensor and a standard ELISA protocol.

Sample number	$\mu\text{mol L}^{-1}$, L-serine		$\mu\text{mol L}^{-1}$, D-serine	
	Screening method	ELISA	Screening method	ELISA
1	1.45±0.02	1.42±0.12	3.13± 0.04	3.02±0.12
2	8.77±0.03	8.70±0.14	3.75± 0.02	3.70±0.11
3	204.13±0.02	203.97±0.14	8.98± 0.03	8.90±0.11
4	25.72±0.03	25.17±0.15	6.41 ±0.01	5.97±0.15
5	2.86±0.01	2.85±0.12	1.44± 0.02	1.39±0.19
6	5.35±0.02	5.40±0.13	5.63± 0.01	5.60±0.10
7	27.45±0.03	27.40±0.17	3.56 ±0.02	3.56±0.13
8	26.56±0.02	26.50±0.12	2.35 ±0.01	2.34±0.12
9	6.93±0.01	6.92±0.12	1.11 ±0.02	1.30±0.10
10	10.46±0.03	10.40±0.15	4.32 ±0.02	4.30±0.12
11	9.36±0.02	9.36±0.16	8.53± 0.04	8.49±0.10
12	22.75±0.01	22.15±0.12	9.06± 0.03	9.07±0.15
13	3.11±0.02	3.11±0.13	4.04 ±0.01	3.95±0.1
14	9.83±0.05	9.80±0.13	9.98 ±0.02	9.90±0.17
15	6.12±0.03	6.10±0.20	5.06 ±0.02	5.00±0.17
t-test	2.22		2.19	

The calibration equation recorded for L-serine was: $1/t_{on} = 0.03 + 3.82 \times 10^3 C_{L-serin\grave{a}}$ with a correlation coefficient r of 0.9999. The linear concentration range was between 1×10^{-12} și $1 \times 10^{-3} \text{ mol L}^{-1}$, with a limit of determination $1 \times 10^{-12} \text{ mol L}^{-1}$.

The range is able to cover L-serine concentrations in healthy individuals and breast cancer patients.

The calibration equation recorded for D-serine was: $1/t_{on} = 0.03 + 4.71 \times 10^{10} C_{D-serin\grave{a}}$, with a correlation coefficient r of 0.9995. The linear concentration range was between $1 \times 10^{-14} \text{ mol L}^{-1}$. The range is able to cover the concentration of D-serine in breast cancer patients.

3.3.1.2. L- and D-leucine

Stochastic mode was used to determine the response characteristics of enantioselective stochastic sensors. The response characteristics are shown in Table 3.2.

Table 3.2. Response characteristics for enantioselective stochastic sensors used for leucine enantioselectivity analysis.

Stochastic sensor based on N-methyl-fulleropyrrolidine &	Leucine	Signature $t_{off}(s)$	Equation of calibration ¹ , R	Sensitivity, $s^{-1} g^{-1} L$	Limit of determination, $ag L^{-1}$	Linear concentration range, $g L^{-1}$
Graphite/Fe ₂ O ₃	L	0.6	$1/t_{on} = 0.04 + 8.17 \times 10^{13}C$ r=0.9993	8.17×10^{13}	10.00	$1 \times 10^{-17} - 1 \times 10^{-5}$
	D	0.8	$1/t_{on} = 0.01 + 1.42 \times 10^{13}C$ r=0.9994	1.42×10^{13}	100.00	$1 \times 10^{-16} - 1 \times 10^{-9}$
Nanographene	L	2.2	$1/t_{on} = 0.02 + 3.44 \times 10^{12}C$ r=0.9995	3.44×10^{12}	100.00	$1 \times 10^{-16} - 1 \times 10^{-4}$
	D	0.9	$1/t_{on} = 0.02 + 1.35 \times 10^{15}C$ r=0.9996	1.35×10^{15}	1.00	$1 \times 10^{-18} - 1 \times 10^{-6}$

¹ $\langle C \rangle = mol L^{-1}$; $\langle t_{on} \rangle = s$.

The signatures of the two enantiomers are different when the same stochastic sensor was used, which proves that the sensors are enantioselective and can be used for simultaneous testing of the two enantiomers. The linear concentration ranges are broad, allowing enantioanalysis of leucine in whole blood samples despite the health status of the individuals.

Very low limits of determination ($ag L^{-1}$) were recorded; for the determination of L-leucine, the lowest limit of determination was recorded when using the graphite/Fe₂O₃-based stochastic enantioselective sensor, while for the determination of D-leucine, the lowest limit of determination was recorded for the nanographene-based stochastic enantioselective sensor. L-leucine was determined with the highest sensitivity when the graphite/ Fe₂O₃-based sensor was used, while D-leucine was determined with the highest sensitivity when the nanographene-based sensor was used.

3.3.2. Selectivity of the proposed sensors used for the determination of serine and leucine

3.3.2.1. L- and D-serine

The selectivity of stochastic sensors is given by the values recorded for the signatures of possible interferences; a difference of at least 2 s between the signatures of possible interferences and the signatures of serine enantiomers confirms the selectivity of the stochastic sensor. The following amino acids were tested as possible interferences: L- and D-glutamine, L- and D-tryptophan, L- and D-aspartic acid and L- and D-leucine.

The values recorded for their signatures were: L-glutamine 0.3 s, D-glutamine 0.7 s; L-tryptophan 3.7 s; D-tryptophan 3.3 s; L-aspartic acid 2.1 s; D-aspartic acid 2.5s; leucine 1.5 s, D-leucine 2.8 s. These values showed that the proposed sensor is not only enantioselective but also selective towards these amino acids.

3.3.2.2. L- and D-leucine

The selectivity of the stochastic sensors is given by the difference between the signals (t_{off} values) recorded for leucine enantiomers and those obtained for CA15-3, CEA, HER-2, p53, Ki67, maspin and CA19-9 – the common biomarkers used for breast cancer diagnosis.

Table 3.3. Selectivity of stochastic sensors.

Stochastic sensor based on N-methyl-fulleropyrrolidine &	CA15-3	CEA	HER2	Maspin	Ki67	CA19-9	p53	L-leucine	D-leucine
	Signature (s)								
Graphite/Fe ₂ O ₃	1.1	1.5	2.2	1.9	3.0	2.4	3.5	0.6	0.8
Nanographene	0.2	0.6	3.0	2.5	3.2	2.8	1.7	2.2	0.9

The results presented in Table 3.3, proved that none of the other biomarkers interfere in leucine enantioanalysis, despite the matrix used for the stochastic sensor design. Ten enantioselective stochastic sensors of each of the two types designed for leucine enantioanalysis were constructed. Response characteristics were measured daily for one month. There was no significant change in sensitivity, with a variation of less than 0.15%, demonstrating the reproducibility of the design of each stochastic sensor type. After one month

of measurements, the variation in sensitivities recorded again was less than 1.2%, proving that the sensors are stable for at least one month.

3.3.3. *Enantioanalysis of serine in whole blood samples used for the determination of L- and D-serine*

Serine enantiomers were identified in whole blood sample screening plots using the stochastic enantioselective sensor according to their signatures. Whole blood samples from confirmed breast cancer patients as well as healthy volunteers were screened using the proposed sensor. The results are presented in Tables 3.1 and 3.2

Table 3.4. Whole blood serine assay obtained from healthy volunteers using a stochastic enantioselective sensor and a standard ELISA protocol

Sample number	$\mu\text{mol L}^{-1}$, L-serine	
	Screening method	ELISA
1	209.15 \pm 0.03	209.20 \pm 0.17
2	293.63 \pm 0.03	291.93 \pm 0.17
3	315.40 0.02	314.87 \pm 0.13
4	123.41 \pm 0.03	123.50 \pm 0.15
5	178.65 \pm 0.04	178.79 \pm 0.20
t-test	2.67	

A very good correlation between serine enantiomer concentrations was obtained by the screening method (based on the use of the stochastic enantioselective sensing method) and ELISA (standard method for the analysis of serine enantiomers).

A paired Student's t-test was performed at the 99.00% confidence level (theoretical t-value: 4.032). The calculated t-values for each of the sensors and for each sample type were less than 4.032; these results showed that there was no statically significant difference between the results obtained using the proposed stochastic sensor and ELISA (Tables 3.1 and 3.4). Consequently, the proposed screening method is validated for serine enantioanalysis in whole blood samples. The absence of D-serine in whole blood samples from healthy volunteers may indicate that D-serine is a biomarker capable of being used for early diagnosis of breast cancer. In addition, serine enantioanalysis may be a key factor in the early diagnosis of breast cancer. The main advantages of using the proposed method for serine enantioanalysis were that it can ensure low cost of quantitative and qualitative analysis of L- and D-serine; both enantiomers can be analysed simultaneously, and breast cancer can be identified at a very early stage. No

enzymes were used in the sensor design, which makes the sensor stable over time and has significant reliability advantages.

3.3.4. Enantioanalysis of leucine in whole blood samples used for the determination of L- and D-leucine

Whole blood samples were used as collected from patients, without any processing. Measurements were performed according to the description of the stochastic method above.

After the plots were obtained (Figure 3.3 and 3.4), the L- and D-leucine signatures were identified and after the t_{on} values between the two t_{off} values were read. To validate the sensors, known mixtures of enantiomers (in different proportions) were introduced into whole blood samples and enantiomer recovery was performed (Table 3.5).

Determinations of leucine enantiomer were performed before and after the addition of mixture to calculate the recovery of the known amount added. Table 3.5. L- and D-leucine recovery assays in whole blood samples (N=10).

Table 3.5. shows that high recoveries of enantiomers were obtained in whole blood despite the ratios of L- to D-leucine in whole blood. This proved the high accuracy and reliability of the measurements.

L:D	Recovery, %													
	1:99		1:50		1:25		1:1		25:1		50:1		99:1	
Enantiomer	L	D	L	D	L	D	L	D	L	D	L	D	L	D
Graphite /Fe ₂ O ₃ based sensor	99.10±0.05	96.98±0.02	97.95±0.04	99.18±0.02	99.00±0.02	98.75±0.03	98.82±0.02	98.99±0.01	99.15±0.01	99.10±0.03	99.99±0.01	97.98±0.02	98.16±0.03	99.90±0.02
Nanographene based sensor	99.32±0.02	96.50±0.03	98.00±0.02	99.53±0.03	99.18±0.03	99.65±0.02	98.09±0.01	99.99±0.03	99.13±0.02	99.76±0.02	99.12±0.03	97.00±0.04	97.43±0.02	99.66±0.03

Real whole blood samples collected from confirmed breast cancer patients and healthy volunteers were analyzed using stochastic enantioselective sensors. The results obtained are shown in Table 3.6.

Table 3.6. Enantioanalysis of leucine in whole blood samples (N=10).

PSample No.	State of health	L-leucine, pg mL^{-1}		D-leucine, ng mL^{-1}	
		Graphite/ Fe_2O_3	Nanographene	Graphite/ Fe_2O_3	Nanographene
Stochastic sensor based on N-methyl-fullero-pyrrolidine &					
1	Confirmed with breast cancer	8.62±0.02	8.08±0.01	3.52±0.02	3.30±0.03
2		0.48±0.01	0.49±0.03	5.00±0.03	4.75±0.02
3		8.25±0.01	8.71±0.03	0.20±0.01	0.18±0.02
4		15.48±0.02	16.02±0.03	1.87±0.02	1.69±0.03
5		6.11±0.01	5.50±0.03	1.00±0.02	1.00±0.03
6		1.24±0.03	0.98±0.02	2.00±0.01	2.17±0.02
7		3.47±0.01	2.93±0.02	2.60±0.03	2.58±0.01
8		0.08±0.01	0.07±0.02	33.10±0.02	35.01±0.01
9		2.91±0.01	2.26±0.03	5.23±0.03	5.00±0.01
10		8.30±0.03	8.12±0.01	1.17±0.03	1.18±0.01
1	Healthy volunteers	18.21±0.01	18.34±0.02	-*	-*
2		20.58±0.02	20.84±0.01	-*	-*
3		5.48±0.01	5.12±0.03	-*	-*
4		32.25±0.02	32.40±0.01	-*	-*
5		7.12±0.01	7.15±0.03	-*	-*
6		27.16±0.02	27.19±0.01	-*	-*
7		52.01±0.03	51.15±0.02	-*	-*
8		4.89±0.01	4.68±0.03	-*	-*
9		51.97±0.03	52.53±0.01	-*	-*
10		43.47±0.01	43.50±0.02	-*	-*
t-test		2.96		3.01	

* D-leucine was not found.

A paired Student t-test was conducted at a confidence level of 99.90%. The calculated t-values for each enantiomer of leucine were less than 3.10, indicating that there is no statistically significant difference between the results obtained using the proposed enantioselective stochastic sensors (Table 4), and that enantioselective stochastic sensors can be relied upon for the molecular identification and quantification of L- and D-leucine in whole blood samples. Further, the D-leucine was only found in the samples collected from confirmed patients with breast cancer, and not in the whole blood from healthy volunteers.

3.4. CONCLUSIONS

A stochastic enantioselective sensor was designed and used for screening blood samples for L- and D-serine. Zn(II)-5(4-carboxyphenyl)-10,15,20-tris (4-phenoxyphenyl) porphyrin was used to modify a nanographene paste, which was introduced into a non-conductive plastic tube to obtain the enantioselective stochastic sensor. The sensor had high sensitivity for both enantiomers and also low determination limits.

Validation of the sensor showed that there was a good correlation between the results obtained by proposed detection method and ELISA demonstrating the suitability of the proposed method for serine enantioanalysis in whole blood samples.

In addition this method demonstrated that D-serine can be a biomarker for early diagnosis of breast cancer.

As for leucine, the proposed enantioselective stochastic sensors were found to have outstanding characteristics in biomedical analysis. Their use for screening whole blood samples may bring the screening test very close to the diagnostic test, as D-leucine was found only in confirmed breast cancer patients, and not in healthy volunteers.

CHAPTER IV

STOCK MICROSENSORS BASED ON CARBON NANOPULBER FOR ULTRASENSIBLE DETERMINATION OF CA15-3, CEA AND HER-2 IN WHOLE BLOOD

4.1. INTRODUCTION

CA15-3, CEA and HER-2 play the role of biomarkers that has a prognostic and can facilitate personalized treatment for breast cancer. HER-2 positive breast cancers are considered to be more aggressive than HER-2 negative breast cancers. Numerous methods have been proposed for assaying CA15-3, CEA and HER-2 (Table 4.1). Therefore, this paper proposes two new stochastic microsensors based on carbon nanopowder (nC) modified with gold nanoparticles (AuNp) and two porphyrins -5,10,15,20-tetraphenyl-21H, 23H-porphyrin (TPP) and 5,10,15,20-tetrakis (pentafluorophenyl chloride)-21H, 23H-iron (III) porphyrin [Fe(TPFPP)Cl] – for the simultaneous assay of CEA, CA15-3 and HER-2, as a screening test based on their simultaneous analysis will provide more information about the personal diagnosis and treatment of breast cancer. The novelty of the work, in addition to the new design used for the proposed stochastic microsensors for CEA, CA15-3 and HER-2 assay, is the use of a single instrument for simultaneous assay of the three biomarkers.

The current development mechanism for stochastic sensors is based on channel conductivity: the molecule enters the channel and the current decreases to zero until the entire molecule is inside the channel – the time taken to enter the channel depends on the size, volume, conformation, unfolding capacity (if protein) and velocity determined by the applied potential, and is known as the molecule signature, noted as the t_{off} value on the charts. Meanwhile, redox processes take place in the channel, in a time of equilibrium called the t_{on} on the charts, the tone value is read between two t_{off} values, and this depends on the concentration of the molecule in the biological fluid in which the molecule is determined.

4.2. EXPERIMENTAL PART

4.2.1. Materials and methods

All chemicals were of analytical quality. Deionised water was used to prepare the solutions used in the experiments. All CA15-3, CEA and HER-2 solutions were prepared in phosphate buffer solution (PBS, pH=7.40). The electrochemical cell was composed of three electrodes: the reference electrode (Ag/AgCl), the counter electrode (Pt) and the working electrode (stochastic microsensor). A chronoamperometric method was used to measure the t_{on} and t_{off} values at a constant potential (125 mV vs Ag/AgCl).

For microsensor design: 100 mg of carbon nanopowder was mixed with 10 μ L gold nanoparticle suspension and paraffin oil was added until a paste was obtained. The paste was divided into two equal parts and 50 μ L of one of the following porphyrins were added to each: 5,10,15,20-tetraphenyl-21H, 23H-porphyrin (TPP/AuNp) or 5,10,15,20 – tetrakis (pentafluorophenyl chloride) – 21H, 23H-iron (III) porphyrin (Fe(TPFPP)Cl/AuNp). Silver wire served as the contact between the paste and the external circuit. A chronoamperometric method was used for t_{on} and t_{off} measurements at constant potential (125 mV vs Ag/AgCl). The value of the applied potential (125 mV vs Ag/AgCl) was determined experimentally; potentials between 0.05 and 250 mV were applied; the best form of the stochastic signal was obtained when a potential of 125 mV vs Ag/AgCl was applied. Based on the t_{off} value, the analyte was identified in the charts recorded with the stochastic microsensors, and then the t_{on} value was further cytometrically determined and used to determine the concentration of each biomarker (Figure 4.1). The unknown concentrations of Ca15-3, CEA and HER-2 in whole blood samples were determined from the calibration equations ($1/t_{on} = a + bx_{Cbiomarker}$) recorded with each of the sensors for each of the biomarkers.

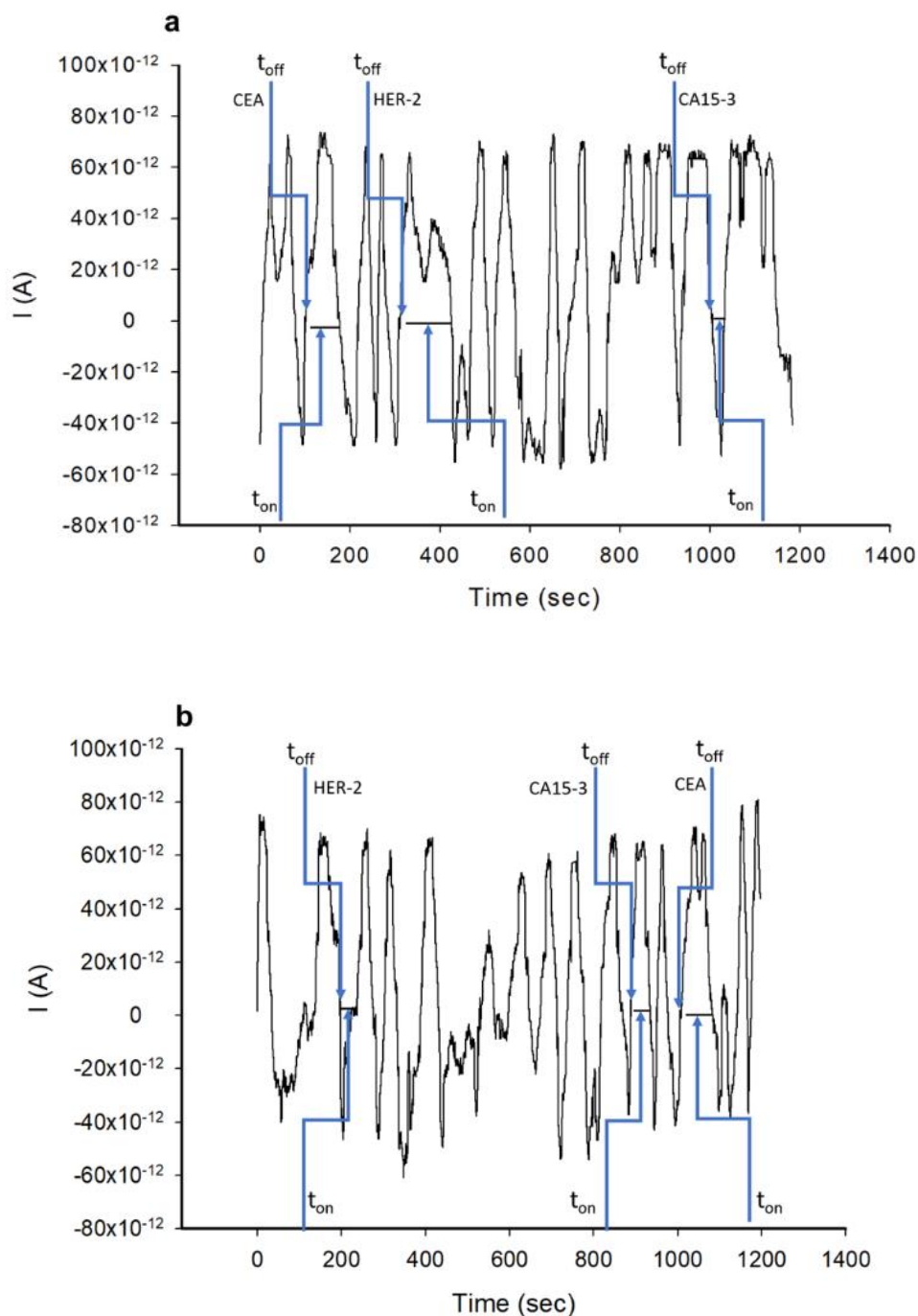


Figure 4.1. Recognition of CA15-3, CEA and HER-2 patterns in whole blood samples using a stochastic microsensor based on (a) Fe(TPFPP)Cl/AuNp and (b) TPP/AuNp. Whole blood samples were obtained from University Hospital Bucharest (with ethics committee approval no. 11/2013). The electrochemical cell was loaded with biological sample and after recording the plot and identifying CA15-3, CEA and HER-2 signatures, the unknown biomarker concentrations in whole blood samples were determined using the stochastic method described above.

4.3. RESULTS AND DISCUSSIONS

4.3.1. Stochastic sensor response characteristics

The response characteristics of the proposed microsensors are shown in Table 4.1. All response characteristics were determined at 25 °C, when a potential of 125 mV versus Ag/AgCl was applied. First, different signatures (t_{off} values) for Ca 15-3, CEA and HER-2 were recorded for each of the stochastic microsensors, proving that the three biomarkers can be determined simultaneously in whole blood samples.

Table 4.1. Response characteristics of stochastic sensors used for CA15-3, CEA and HER-2 testing.

Stochastic microsensor based on nC	Signature t_{off} (s)	Linear concentration range	Calibration equations; correlation coefficient, r^*	Sensitivity	LOQ
Fe(TPFPP)Cl/AuNp	CA15-3*				
	4.7	1.00x10 ⁻⁷ - 1.00x10 ³	1/ t_{on} = 0.03 + 5.80x10 ³ ×C r=0.9998	5.80x10 ³	1.00x10 ⁻⁷
	CEA**				
	0.6	1.28x10 ⁻⁵ - 2.00x10 ⁻¹	1/ t_{on} = 0.04 + 6.16x10×C r=0.9993	6.16x10	1.28x10 ⁻⁵
	HER 2**				
	2.6	3.90x10 ⁻⁹ - 3.90x10 ⁻⁵	1/ t_{on} = 0.02 + 1.43x10 ⁵ ×C r=0.9999	1.43x10 ⁵	3.90x10 ⁻⁹
TPP/AuNp	CA15-3*				
	6.8	1.00x10 ⁻⁷ - 1.00x10 ³	1/ t_{on} = 0.04 + 2.32x10 ³ ×C r=0.9994	2.32x10 ³	1.00x10 ⁻⁷
	CEA**				
	1.9	1.00x10 ⁻⁷ - 1.00	1/ t_{on} = 0.03 + 1.90x10 ⁴ ×C r=0.9997	1.90x10 ⁴	1.00x10 ⁻⁷
	HER 2**				
	1.3	3.50x10 ⁻⁸ - 3.90x10 ⁻⁵	1/ t_{on} = 0.03 + 3.53x10 ⁴ ×C r=0.9986	3.53x10 ⁴	3.50x10 ⁻⁸

*<C>= U mL⁻¹; < t_{on} >=s; <Sensitivity> = s⁻¹ U⁻¹ mL; **<C>= µg mL⁻¹; < t_{on} >=s; <Sensitivity> = s⁻¹ µg⁻¹ mL; LOQ - limit of quantification

All linear concentration ranges are wide, making it possible to determine these biomarkers at any stage of breast cancer.

Sensitivity is also very high. Higher sensitivities were recorded for CEA and HER-2 testing when the TPP/AuNp based sensor was used. In comparison with the most recent sensors used for CA15-3, CEA and HER-2 testing (Table 4.1), it can be concluded that the TPP/AuNp-based sensor showed the lowest limit of determination (order of magnitude fg mL^{-1}) and for HER-2 testing, the Fe(TPFPP)Cl/AuNp-based sensor showed the lowest limit of determination. For Ca 15-3 testing, although the limits of determination are higher than previously reported [288-290], the proposed sensors can be used for CA15-3 testing without the need for any sample processing the linear concentration range covers breast cancer patients at any stage of disease.

The advantages of the proposed sensors over those presented in Table 4.1 are also the following: they can perform simultaneous detection of all three biomarkers; no sampling is required prior to measurement; reliable qualitative analysis of each biomarker is immediately followed by analysis of that biomarker.

4.3.2. Stability and reproducibility measurements

Ten stochastic sensors for each of the two types were designed [TPP/AuNp and Fe(TPFPP)Cl/AuNp] and measurements were performed daily for one month.

The measurement for each sensor type showed no significant change in sensitivity, with the variation in sensitivity for each type being less than 0.12%; this proved the reproducibility of the design of each stochastic sensor type. After 30 days of measurements, the variation in sensitivities recorded for the TPP/AuNp based stochastic sensor was less than 0.11%, while for the Fe(TPFPP)Cl/AuNp based stochastic sensor it was less than 0.08%; this proved that the sensors are stable for at least one month when daily measurements are performed.

4.3.3. Selectivity of stochastic microsensors

The selectivity of stochastic microsensors is given by the difference between the signatures (t_{off} values) recorded for Ca15-3, CEA and HER-2 and those obtained for other biomarkers/substances in biological samples. Possible interfering species selected were p53, Ki67, mpsin, CA19-9, ascorbic acid, dopamine and uric acid.

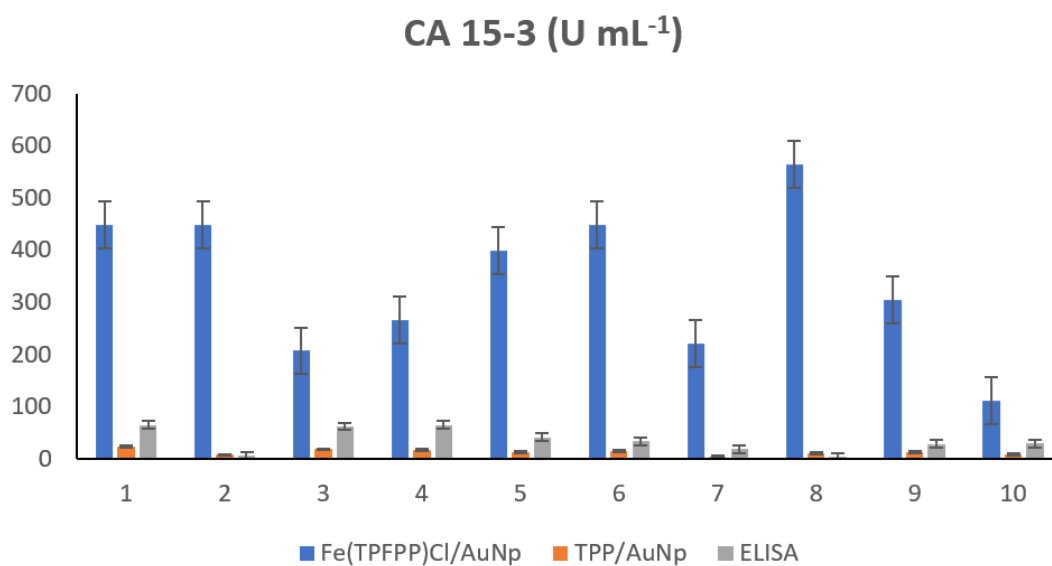
The results presented in Table 4.2 demonstrated that none of the putative interfering species interfered with the simultaneous analysis of CA15-3, CEA and HER-2.

Table 4.2. Selectivity of stochastic micro-sensors.

Stochastic microsensor based on nC	Signature (s)									
	CA15-3	CEA	HER2	Maspin	Ki67	CA19-9	p53	Ascorbic acid	Dopamine	Uric acid
Fe(TPFPP)Cl/AuNp	4.7	0.6	2.6	2.0	1.3	3.0	3.5	0.2	1.7	3.2
TPP/AuNp	6.8	1.9	1.3	2.3	3.2	2.5	0.8	0.4	1.5	0.2

4.3.4. Simultaneous ultrasensitive determination of CA15-3, CEA and HER-2 in whole blood

Ten whole blood samples from patients confirmed with breast cancer were examined using the two stochastic microsensors. Shortly after reading the t_{off} values, the corresponding t_{on} values were read. The t_{on} values were used to determine the concentrations of CA15-3, CEA and HER-2 whole blood samples according to the stochastic method described above. The results obtained from the screening of whole blood samples are shown in table 4.2 and Figure 4.2.



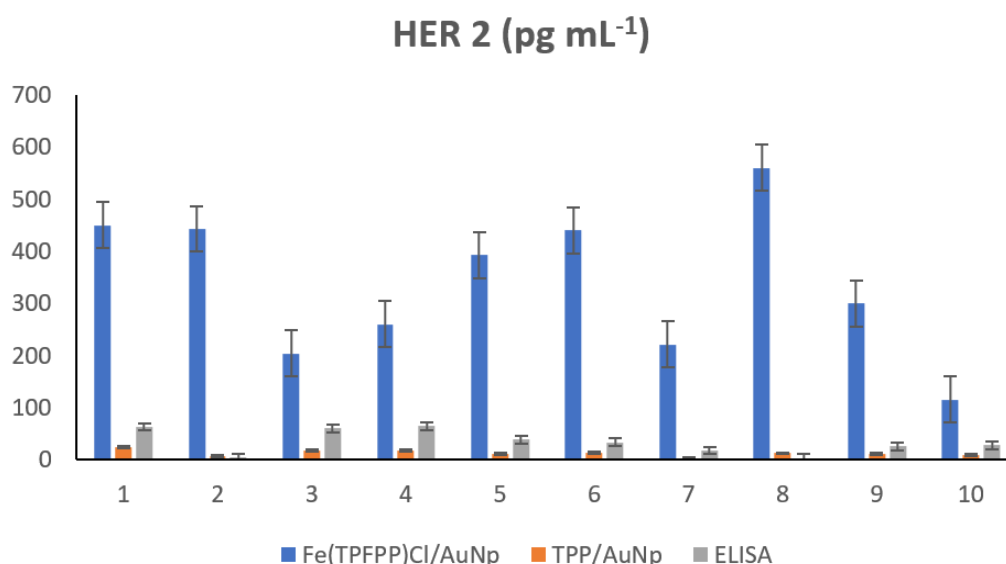
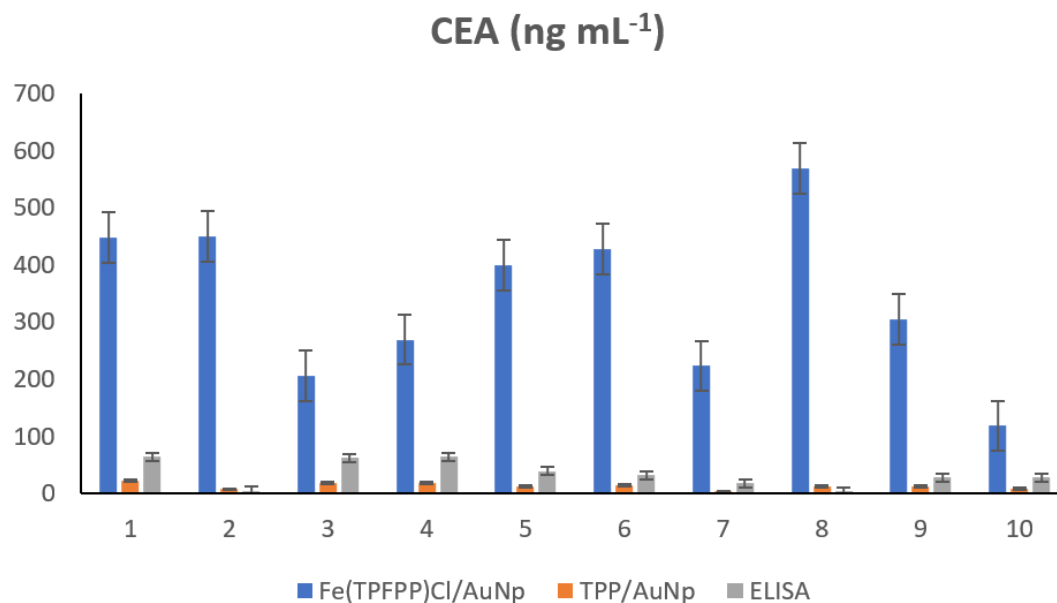


Figure 4.2. Quantitative determination of (a) CA15-3, (b) CEA and (c) HER-2 in whole blood samples using stochastic: Fe(TPFPP)Cl/AuNp and TPP/AuNp based microsensors and standard ELISA.

Very good correlations were obtained between the results obtained using the two stochastic microsensors. A t-test at 99.00% confidence level (tabulated theoretical t-value: 4.032) was also performed for each biomarker. All calculated t-values were than the tabulated value, proving that there is no statistically significant difference between the results obtained using the two stochastic microsensors and ELISA (the standard test, the method used for testing these biomarkers in whole blood samples) (Table 4.2 and Figure 4.2). Consequently, the

proposed stochastic microsensors can be reliably used for the simulated ultrasensitive determination of CA15-3, CEA and HER-2 in whole blood samples.

4.4. CONCLUSIONS

The proposed stochastic microsensors were used for simultaneous testing of CA15-3, CEA and HER-2 in whole blood samples. Their linear working concentration ranges cover breast cancer patients at any stage of the disease, and determinations are performed with high sensitivity. The screening test based on the use of the two microsensors as performed with high sensitivity. The screening test based on the use of the two microsensors as screening tools can be used for early detection of breast cancer, for determining the need for personalized treatment, and for determining the effectiveness of breast cancer treatment.

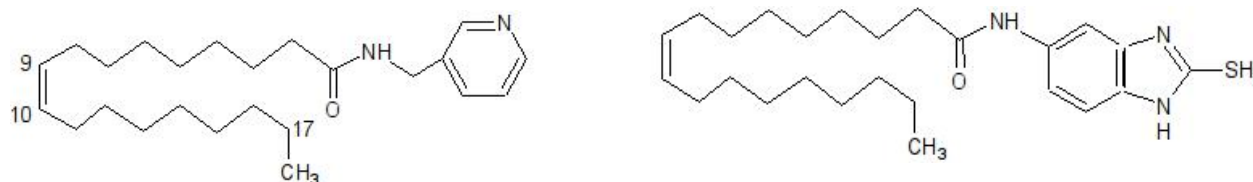
CHAPTER V

ULTRASENSIBLE TESTING OF HER-1, HER-2 AND HEREGULIN- α IN WHOLE BLOOD

5.1. INTRODUCTION

HER-1, HER-2 and heregulin- α have served as prognostic biomarkers, but can also be used to facilitate personalized treatment. Apart from standard methods based on the use of ELISA (enzyme-linked immunosorbent assay) for testing HER-1, HER-2 and heregulin- α , different methods of analysis have been proposed. Due to the importance of simultaneous testing of HER-1, HER-2 and heregulin- α in biological samples, there is a real need to develop rapid and ultrasensitive screening methods for their determination in a single run (simultaneously) in real samples. Therefore, in this work, we proposed two stochastic microsensors based on physically immobilized oleamide in spheroidal copper-decorated nanographene paste for simultaneous HER-1, HER-2 and heregulin- α testing in whole blood samples.

The novelty of the work is the simultaneous assay of HER-1, HER-2 and heregulin- α and the use of oleamides as modifiers of spheroidal copper-decorated nanographene pastes. The Oleamides selected for ultrasensitive HER-1, HER-2 and heregulin- α dosing were: HER-1, HER-2 and heregulin- α : N-(pyridine-3-yl-methyl) oleamide (O1) and N-(2-mercapto-1H-benzo[d]imidazole-5-yl) oleamide (O2) (Figure 5.1).



(a)

(b)

Figure 5.1. The structures of (a) N-(pyridine-3-yl-methyl) oleamide (O1), and (b) N-(2-mercapto-1H-benzo[d]imidazole-5-yl) oleamide (O2).

5.2. EXPERIMENTAL PART

5.2.1. Materials and reagents

All chemicals were of analytical quality. Deionising water was used to prepare the solutions used in the experiments. All HER-1, HER-2 and heregulin- α solutions were prepared in phosphate buffer solution (PBS, pH=7.40). When not in use, solutions were kept at -20°C .

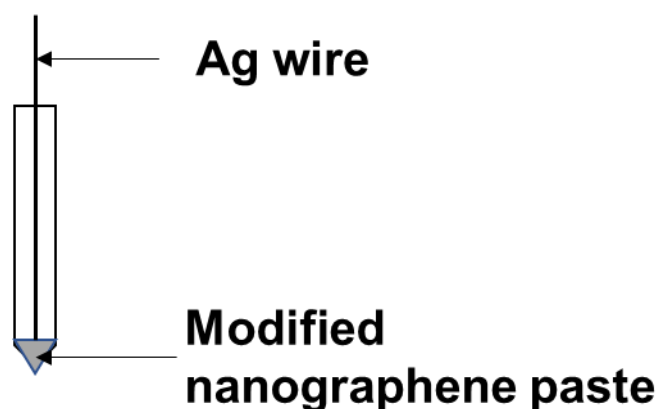
5.2.2. Apparatus and methods

All electrochemical measurements of HER-1, HER-2 and heregulin- α solutions and whole blood samples were performed by connecting to a computer running GPES software.

The electrochemical cell was composed of three electrodes: the reference electrode (Ag/AgCl), the counter electrode (Pt) and the working electrode (stochastic microsensor). All measurements were performed at -25°C . A chronoamperometric method was used to measure the t_{on} and t_{off} values at a constant potential (125 mV vs. Ag/AgCl).

5.2.3. Design of the stochastic microsensors

100 mg of nanographene powder was physically mixed with 10 mg of spheroidal copper. Nanographene, compared to graphene oxide, provides a better surface area for the channels formed by the modifier (oleamide); in addition, there is an increase in surface area which influences the sensitivity of the sensor. The ameter was divided into two equal parts and 50 μL of O1, respectively O2 ($10^{-3} \text{ mol L}^{-1}$) solution was added to each part. Each modified paste was placed in a non-conductive plastic tube printed using a 3D printer in our lab, with an inner diameter of 50 μm and a length of 5 mm (Scheme 5.1).



Scheme 5.1. The design of the stochastic microsensor

5.2.4. Recommended procedures: stochastic method

All measurements were carried out at 25°C . A chronoamperometric method at constant potential (125 mV vs Ag/AgCl) was used for t_{on} and t_{off} measurements. Based on the t_{off} value, the analyte was identified in the charts recorded with the stochastic microsensors, and then the

t_{on} value was read and used for the concentration determination (Figure 5.2). The unknown concentration of HER-1, HER-2 and heregulin- α in whole blood samples were determined from the calibration equation $1/t_{on} = a+bxC_{biomarker}$ recorded with each sensor for each biomarker.

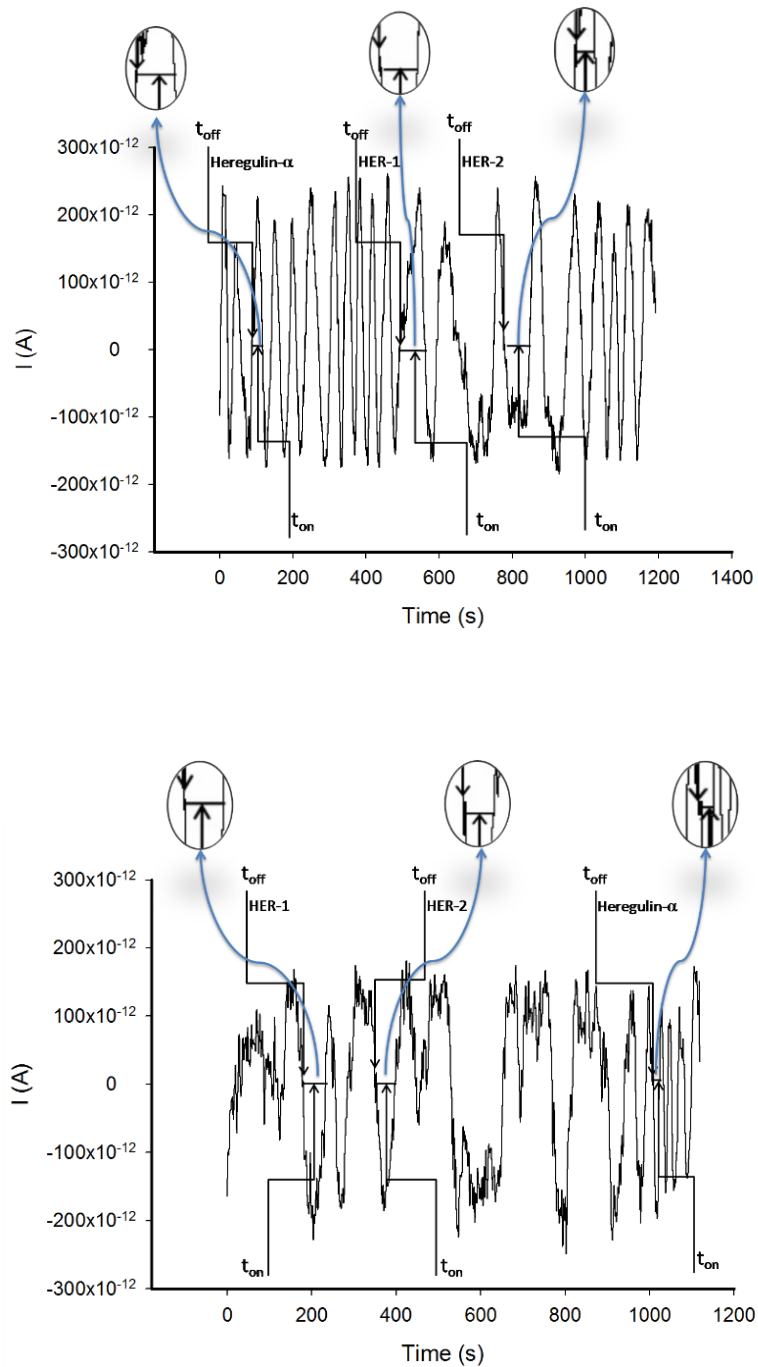


Figure 5.2. Pattern recognition of HER1, HER2, and heregulin- α in whole blood samples, using stochastic microsensors based on nanographene decorated with spheroidal Cu and a) N-(pyridine-3-yl-methyl) oleamide (O1), and (b) N-(2-mercapto-1H-benzo[d]imidazole-5-yl) oleamide (O2).

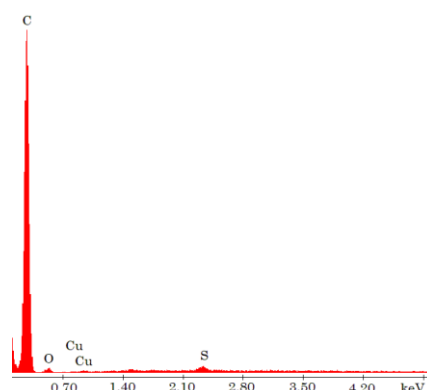
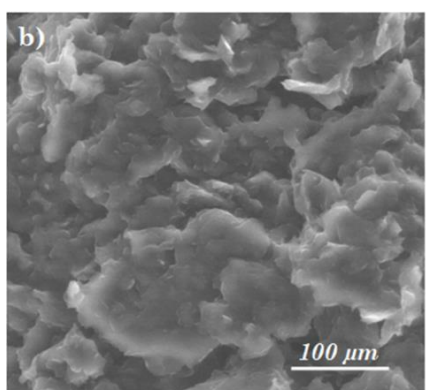
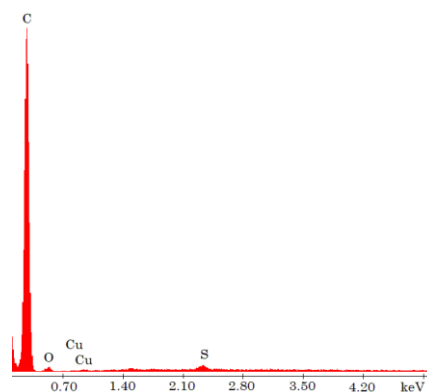
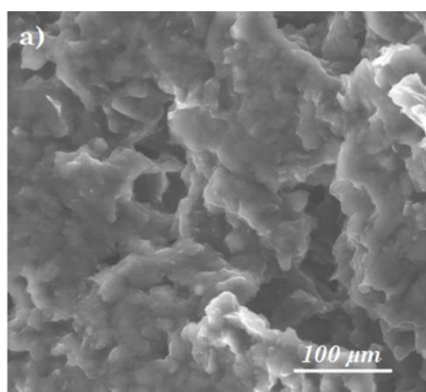
5.2.5. Samples

Whole blood samples were obtained from Bucharest University Hospital (ethics committee approval no. 11/2013). These samples were obtained from patients confirmed with breast cancer. The electrochemical cell was loaded with the biological sample and, after charting and identifying HER-1, HER-2 and heregulin- α signatures, the unknown biomarker concentration in whole samples were determined using the stochastic method described above.

5.3. RESULTS AND DISCUSSIONS

5.3.1. Morphological characterization and structure of pastes used for stochastic microsensor design

Figure 5.3. reveals the morphology of the analysed samokes and elemental analysis by EDX technique. From the qualitative analysis of the spheroidal copper-modified nanographene, spherical particles embedded in the organic matrix can be observed (Figure 5.3 (a)). The addition of oleamide O1 and O2 (Figure 5.3(b) and (c)) facilitated the presence of the necessary channels/pores in the stochastic analysis mehod for stochastic signal development. Semiquantitative EDX analysis showed that the relevant elemental is C (98.6% by weight), followed by O (0.64% by weight), Cu (0.43% by weight) and S(0.33% by weight).



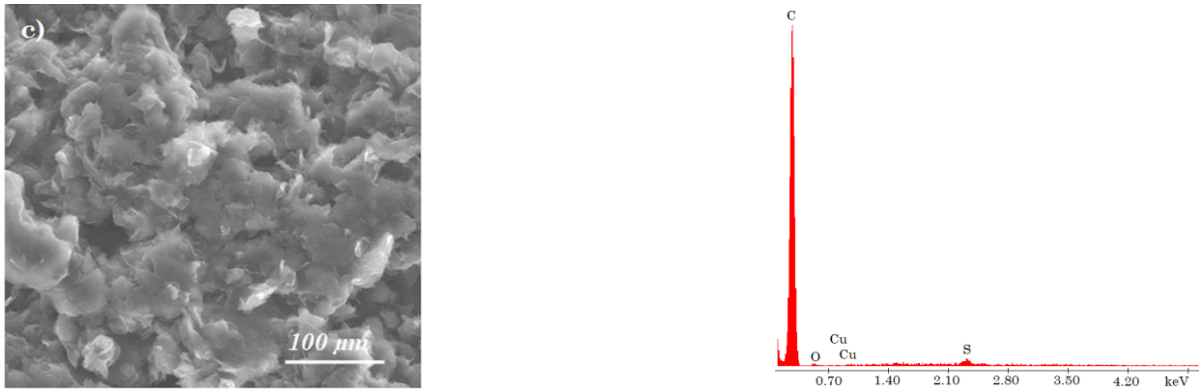


Figure 5.3. SEM images and EDX spectra of (a) the paste containing nanographene and spheroidal Cu; (b) the paste containing nanographene and spheroidal Cu modified with O1; (c) the paste containing nanographene and spheroidal Cu modified with O2.

5.3.2. Response characteristics of the stochastic microsensors

A potential of 125mV was applied and the biomarkers go one by one into the oleamide pore. As they enter the pore, the pore blocks it and the current drops to 0 A. The time spent in this step is called the biomarker signature and is given by the t_{off} value. In the next step, the biomarker undergoes binding processes as well as redox processes – the time spent for these processes is known as the t_{off} – and used for quantitative measurements.

Table 5.1. Response characteristics of the stochastic microsensors when used for the determination of HER1, HER2 and heregulin- α .

Microsenzor stochastic pe bază de nanografene, Cu sferoidal și	Semnătură t_{off} (s)	Domeniu linear de concentrație (g mL^{-1})	Ecuatie de calibrare; coeficient de corelație, r^*	Sensibilitate ($\text{s } \mu\text{g mL}^{-1}$)	LOQ (pg mL^{-1})
O1	1.2	3.90×10^{-13} - 3.90×10^{-8}	HER 1		
			$1/t_{\text{on}} = 0.03 + 7.99 \times C$	7.99	0.39
			$r = 0.9998$		
	4.2	3.90×10^{-12} - 3.90×10^{-10}	HER 2		
			$1/t_{\text{on}} = 0.01 + 1.55 \times 10^2 \times C$	1.55×10^2	3.90
			$r = 0.9993$		
2.3	2.56×10^{-12} - 6.40×10^{-11}	Heregulin- α			
		$1/t_{\text{on}} = 0.15 + 3.01 \times 10^3 \times C$	3.01×10^3	2.56	
		$r = 0.9998$			
O2	1.2	3.90×10^{-11} - 3.90×10^{-8}	HER 1		
			$1/t_{\text{on}} = 0.05 + 9.97 \times C$	9.97	39
			$r = 0.9998$		
	3.4	3.90×10^{-12} - 3.90×10^{-10}	HER 2		
			$1/t_{\text{on}} = 0.01 + 1.10 \times 10^2 \times C$	1.10×10^2	3.90
			$r = 0.9999$		
2.3	5.12×10^{-13} - 1.28×10^{-11}	Heregulin- α			
		$1/t_{\text{on}} = 0.01 + 4.30 \times 10^4 \times C$	4.30×10^4	0.51	
		$r = 0.9999$			

* $\langle C \rangle = \mu\text{g mL}^{-1}$; $\langle t_{\text{on}} \rangle = \text{s}$; LOQ - limit of quantification.

First of all, different signatures (t_{off} values) were recorded for the HER1, HER2, and heregulin- α for each of the stochastic microsensors proving that the three biomarkers can be determined simultaneously in whole blood samples.

Comparable sensitivities (as magnitude order) were recorded for both microsensors when used for the assay of HER-1, and HER-2. A higher magnitude order (10^4) was recorded for the sensitivity of the microsensor based on O2, when heregulin- α was analysed.

A wider working concentration range was recorded for the assay of HER-1, when the microsensor based on O1 was used. For the assay of HER-2, the same working concentration range was recorded for both sensors, while for the assay of heregulin- α , a wider linear concentration range was obtained for the microsensor based on O2.

The lowest limit of quantification for HER-1 was obtained when the microsensor based on O1 was used, while the lowest limit of quantification for heregulin- α was obtained using the microsensor based on O2. The same value was obtained using both microsensors, when used for the assay of HER-2. Accordingly, the stochastic microsensor of choice is the one based on O2.

The reliability of the design as well as the stability in time of the proposed microsensors were evaluated. Ten of each type of microsensors were designed and used for 1 month for the assay of HER-1, HER-2, and heregulin- α . In this period of time, the sensitivities for HER-1, HER-2, and heregulin- α were recorded. For each type of microsensor, the measurements performed during one day showed that the RSD% values for the variation of the sensitivities recorded for 10 microsensors were 0.12% for HER-1, 0.09% for HER-2, and 0.07% for heregulin- α despite the type of microsensor, proving a highly reliable (reproducible) design of the proposed stochastic microsensors. When used for 1 month, the sensitivities variations were 0.21% for the assay of HER-1, 0.25% for the assay of HER-2, and 0.18% for the assay of heregulin- α despite the type of microsensor, proving the stability of the microsensors in time.

5.3.3. Stability and reproducibility measurements

Ten sensors of each of the two types (based on O1 and O2) were designed and daily measurements were taken for one month. Measurements for each sensor type showed no significant change in sensitivity, with the variation for each type being less than 0.30%; this proved the reproducibility of the design of each stochastic sensor type. After 30 days of measurements, the variation in sensitivities recorded for the O1-based stochastic sensor was less than 0.10%, while for the O2-based stochastic sensor it was less than 0.15%; this proved that the sensors are stable for at least one month when daily measurements are performed.

5.3.4. Selectivity

The selectivity of the stochastic microsensors is given by the difference between the signatures (t_{off} values) recorded for HER1, HER2, and heregulin- α and those obtained for other

biomarkers/substances from the biological samples. The possible interfering species selected were: p53, CEA, maspin, and CA19-9.

Table 5.2. Selectivity of the stochastic microsensors used for the determination of HER1, HER2, and heregulin- α .

Stochastic microsensor based on nanographene, spheroidal Cu and	Maspin, Signature (s)	CEA, Signature (s)	CA19-9, Signature (s)	p53, Signature (s)
O1	0.5	1.7	2.9	3.3
O2	0.7	1.9	3.7	4.2

The results shown in Table 2 proved that maspin, CEA, CA19-9, and p53 did not interfere in the determination of HER1, HER2, and heregulin- α .

5.3.5. Ultrasensitive simultaneous determination of HER-1, HER-2 and heregulin- α in whole blood

Eleven whole blood samples from patients confirmed with breast cancer were screened using the two stochastic microsensors. Pattern recognition was done first – based on the identification of the t_{off} value (signature) specific to HER1, HER2, and heregulin- α in the diagrams obtained using the proposed stochastic microsensors (Figure 5.2). Just after reading the t_{off} values, in between two t_{off} values, the corresponding t_{on} values were read. The t_{on} values were used to determine the concentrations of HER1, HER2, and heregulin- α in the whole blood samples, accordingly with the stochastic method described above. The results obtained after the screening of whole blood samples are shown in Table 5.3.

Table 5.3. Rezultatele obținute pentru testul ultrasensibil al HER-1, HER-2 și heregulin- α în sângele integral, utilizând microsenzori stocastici (N=10).

Sample No.	pg mL ⁻¹ , HER 1		pg mL ⁻¹ , HER 2		pg mL ⁻¹ , Heregulin- α	
	Stochastic microsensors based on nanographene, spheroidal Cu and					
	O1	O2	O1	O2	O1	O2
1	1.93±0.02	1.97±0.03	193.75±0.04	192.04±0.03	1.36±0.02	1.15±0.03
2	5.87±0.03	6.12±0.02	169.79±0.03	169.97±0.05	2.48±0.03	2.44±0.02
3	3.48±0.03	3.50±0.03	256.24±0.05	251.08±0.04	3.76±0.03	3.25±0.02
4	0.92±0.03	0.99±0.01	224.65±0.03	227.09±0.05	0.97±0.04	1.01±0.01
5	3.49±0.01	3.23±0.03	528.13±0.05	531.25±0.05	1.49±0.01	1.92±0.02
6	5.87±0.03	5.30±0.03	256.20±0.03	258.43±0.04	0.93±0.01	0.89±0.02
7	1.90±0.02	1.98±0.01	357.16±0.04	359.81±0.05	0.63±0.02	0.60±0.03
8	1.89±0.02	1.92±0.02	222.65±0.05	229.81±0.05	1.55±0.02	1.34±0.01
9	5.87±0.03	5.90±0.04	195.01±0.04	197.78±0.03	2.48±0.01	2.46±0.02
10	3.47±0.04	3.19±0.02	192.51±0.03	194.30±0.05	1.59±0.02	1.92±0.01
11	0.89±0.01	0.92±0.02	221.14±0.05	221.03±0.03	1.50±0.02	1.58±0.01
t-test	2.57		2.43		2.17	

Very good correlations between the results obtained using the two stochastic microsensors were obtained. Paired t-test was also performed at 99.00% confidence level (tabulated theoretical t-value: 4.032) for each biomarker. All calculated t-values were less than the tabulated value, proving that there is no statistically significant difference between the results obtained using the two stochastic microsensors (Table 5.3). Accordingly, the proposed stochastic microsensors can be reliably used for the ultrasensitive simultaneous determination of HER1, HER2, and heregulin- α in whole blood samples.

5.4. CONCLUSIONS

Two stochastic microsensors based on spheroidal copper-decorated nanographene modified with N-(pyridine-3-yl-methyl) oleamide and N-(2-mercapto-1H-benzo[d]imidazol-5-yl) oleamide were successfully used for the ultrasensitive determination of HER-1, HER-2 and heregulin- α in whole blood samples.

The main feature of the sensors is their use as new tools in screening tests of whole blood and tissue samples for breast cancer.

CHAPTER VI

ULTRASENSITIVE TESTING OF 8-HYDROXY-2'-DEOXYGUANOSINE IN WHOLE BLOOD USING CARBON NANOTUBE-BASED STOCHASTIC MICROSENSORS

6.1. INTRODUCTION

8-Hydroxy-2'-deoxyguanosine (8-OHdG) is used to estimate DNA damage in humans after exposure to cancer-causing agents such as tobacco smoke, asbestos fibres, heavy metals and polycyclic aromatic hydrocarbons. 8-OHdG is a critical biomarker for carcinogenesis [327] and a discriminatory biomarker for early detection of breast cancer [328,329]. Levels of 8-OHdG indicate the stage and type of breast cancer and can be expressed as pmol mg⁻¹ ADN (0.25 for normal breast, 0.98 for benign tumours and 2.44 for malignant tumours [329]) or as pg mL⁻¹ (90,8 for normal breast, 302 for benign tumours and 552 for malignant tumours, also 810 for stage I, 510 for stage II, 380 for stage III and 190 for stage IV [328]). So far, high-performance liquid chromatography [330, 331] as well as enzyme-linked immunosorbent assay [330] and optical [332] and electrochemical [333] sensors have been proposed for the determination of 8-OHdG in biological samples.

Two stochastic microsensors based on single-walled (SWCNT) and multi-walled (MWCNT) carbon nanotube pastes modified with α -cyclodextrin (α -CD) have been proposed for the determination of 8-Hydroxy-2'-deoxyguanine in whole blood. The principle of 8-OHdG determination in whole blood is based on current conductivity: in the qualitative analysis step, the biomarker entering the channel, blocks it, and the current decreases to zero value until the whole biomarker molecule enters the channel (biomarker signature is defined as the t_{off} value); the quantification step takes place inside the channel – when binding processes with the channel pre-tunnel as well as redox processes take place – the t_{on} is the measured value (between 2 t_{off} values) in the charts, and its value is related to the concentration of 8-OHdG in the biological samples.

The selection of SWCNT and MWCNT as matrices was made because they are very stable structures that can keep the channels in stable shape. α -CD was used as a modifier because its shape can provide the necessary channels for stochastic detection.

6.2. EXPERIMENTAL PART

6.2.1. Materials, methods and reagents

SWCNT, MWCNT, α -CD, and the components required for the preparation of the buffer solution (pH=7.5). The serial dilution method was used to obtain solutions of 8-OHdG with concentrations between 1×10^{-15} și 1×10^{-2} g mL⁻¹ required for the determination of the response characteristics of stochastic sensors.

6.2.2. Stochastic microsensor design

100mg of each of the SWCNT and MWCNT were mixed with paraffin oil to form homogeneous pastes. To each of the pastes were added 100 μ L of a 1×10^{-3} mol L⁻¹ solution of α -CD to form the modified pastes. Each of the pastes was placed in a 3D tube printed in our laboratory using the 3D printer, having an internal diameter of the active side of the microsensor of 25 μ . The electrical contact with the external circuit was established using a Ag wire. When not in use, the stochastic microsensors were placed in a dry box.

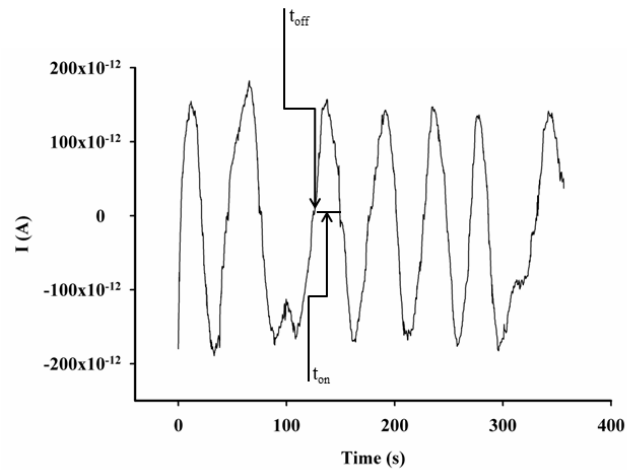
6.2.3. Apparatus

The electrochemical cell comprised the stochastic microsensor (as working sensor), a Ag/AgCl reference electrode, and a Pt wire as auxiliary electrode. All measurements were performed at 125mV vs Ag/AgCl, and at 25°C.

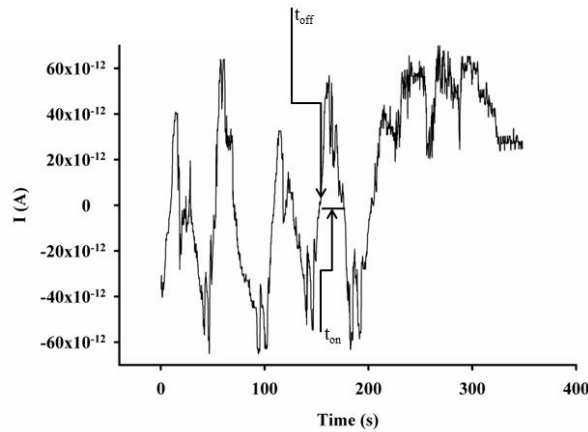
The morphology of the studied pastes based on alpha-CD MWCNT and alpha-CD SWCNT were investigated using scanning electron microscopy (SEM) (Inspect S, FEI Company, The Netherlands). In order to obtain a good resolution of the microscopy images, the pastes were analyzed using the LFD detector (low vacuum), at a high voltage (HV) of 30 kV, and magnification of 1600X.

6.2.4. Stochastics method

A chronoamperometric method at constant potential (125 mV vs Ag/AgCl) was used for t_{on} și t_{off} measurements. Based on the t_{off} value, 8-OHdG was identified in the charts recorded with the stochastic microsensors and subsequently its t_{on} value was read and used for the determination of 8-OHdG concentrations in whole blood samples were determined from the calibration equation $1/t_{on} = a + bxC_{8-OHdG}$ recorded with each of the 8-OHdG sensors. Parameters a and b in the calibration equations were determined by linear regression method.



(a) SWCNT



(b) MWCNT

Figure 6.1. Examples of diagrams obtained for the screening of whole blood samples using the stochastic microsensors based on a) SWCNT, and b) MWCNT

6.2.5. Try

Whole blood samples were obtained from Bucharest University Hospital (ethics committee approval no.11/2013). The electrochemical cell was loaded with the biological sample and, after recording the chart and identifying the 8-OHdG signatures, the unknown 8-OHdG concentrations, the unknown 8-OHdG concentrations in the whole blood samples were determined using the stochastic method described above.

6.3. RESULTS AND DISCUSSIONS

6.3.1. Morphology of the active surface of the stochastic microsensors

Figure 6.2. reports SEM images of α -CD MWCNT (a) and α -CD SWCNT (b). Agglomerations of particles and channels in asymmetric formations can be observed.

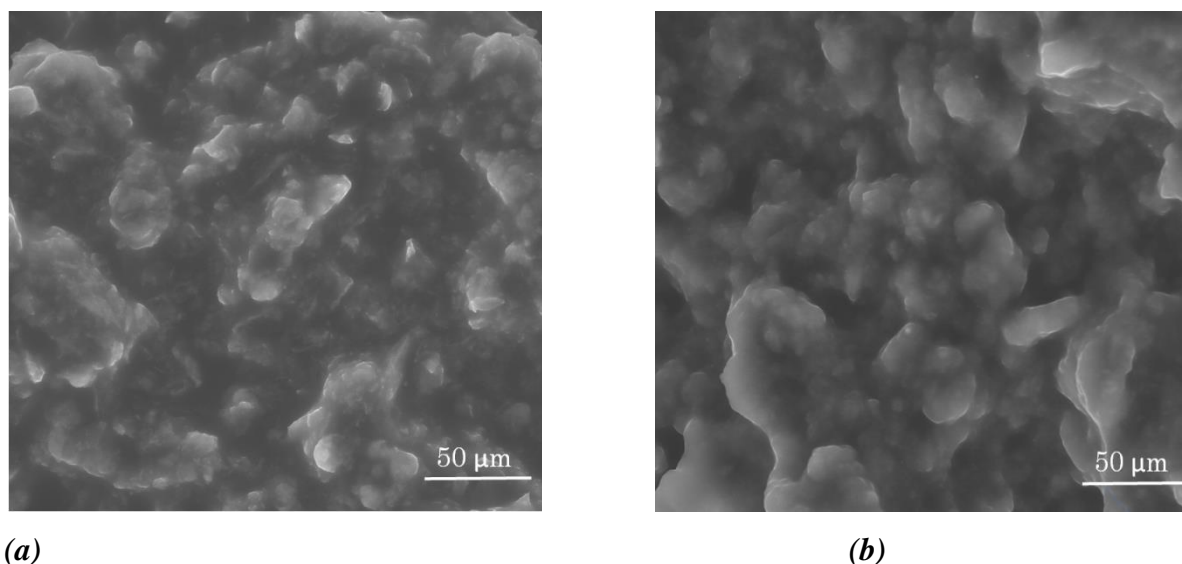


Figure 6.2. SEM images for α -CD MWCNT (a) și α -CD SWCNT (b)

Caracteristicile de răspuns ale senzorilor sunt prezentate în Tabelul 6.1.

Table 6.1. Response characteristics of the stochastic microsensors based on CNT and α -CD

Stochastic microsensor based on α -CD and	Signature t_{off} , s	Equation of calibration * R	Linear conc. range g mL^{-1}	Sensitivity, $\text{s}^{-1} \text{g}^{-1} \text{mL}$	Limit of determination g mL^{-1}
SWCNT	1.2	$1/t_{\text{on}}=0.03+2.64 \times 10^4 C$ $r=0.9999$	1×10^{-12} - 1×10^{-6}	2.64×10^4	1×10^{-12}
MWCNT	0.7	$1/t_{\text{on}}=0.07+7.38 \times 10^7 C$ $r=0.9998$	1×10^{-12} - 1×10^{-8}	7.38×10^7	1×10^{-12}

$$\langle C \rangle = \text{g mL}^{-1} \quad \langle t_{\text{off}} \rangle = \text{s}$$

The wider linear concentration range (1×10^{-12} - $1 \times 10^{-6} \text{ mg L}^{-1}$) was recorded when the microsensor based on SWCNT was used, while the highest sensitivity ($7.38 \times 10^7 \text{ s}^{-1} \text{ g}^{-1} \text{ mL}$) was recorded when the microsensor based on MWCNT was used. The type of carbon nanotube (SWCNT/MWCNT) was not influencing the limit of determination of 8-OHdG ($1 \times 10^{-12} \text{ mg L}^{-1}$). Comparing with the electrochemical sensor proposed by Thanghatthanarungruang et al. [7] that report a linear concentration range 1×10^{-6} - $5 \times 10^{-5} \text{ mol L}^{-1}$, and a limit of determination of $3.06 \times 10^{-7} \text{ mol L}^{-1}$, the proposed sensors from this article shown wider linear concentration ranges, and lower limits of determination.

The reliability of the design as well as the stability in time of the stochastic microsensors were evaluated. Ten of each type of microsensors were designed and used for 1 month for the assay of 8-OHdG. In this period of time, the sensitivities for 8-OHdG were recorded. For each

type of microsensor, the measurements performed during one day showed that the RSD% values for the variation of the sensitivities recorded for 10 microsensors were 0.10% for the microsensor based on SWCNT, and 0.05% for the microsensor based on MWCNT, proving that the design of the stochastic microsensors is reliable. When used for 1 month, the sensitivities variations were 0.15% when the microsensor based on SWCNT was used and 0.08% when the microsensor based on MWCNT was used, proving the stability of the microsensors in time.

6.3.2. Ultrasensitive determination of 8-OHdG in whole blood

Ten whole blood samples from patients confirmed with breast cancer were screened using the two stochastic microsensors. Pattern recognition was done first – based on the identification of the t_{off} value (signature) specific to 8-OHdG in the diagrams obtained using the proposed stochastic microsensors (Figure 1). Just after reading the t_{off} values, in between two t_{off} values, the corresponding t_{on} values were read. The t_{on} values were used to determine the concentrations of 8-OHdG in the whole blood samples, accordingly with the stochastic method described above. The results obtained after the screening of whole blood samples are shown in Table 2.

Table 6.2. Determination of 8-hydroxy-2'-deoxyguanosine in whole blood samples

Sample No	8-hydroxy-2'-deoxyguanosine, pg mL ⁻¹		
	Stochastic microsensor based on α -CD and		ELISA
	SWCNT	MWCNT	
1	198.02±0.02	201.00±0.03	200.03±0.14
2	150.08±0.01	155.30±0.03	151.47±0.12
3	488.18±0.02	487.43±0.01	485.95±0.11
4	184.24±0.01	184.15±0.02	184.00±0.13
5	185.95±0.03	186.00±0.01	184.32±0.12
6	366.12±0.01	363.99±0.03	364.02±0.15
7	287.46±0.02	288.03±0.01	287.95±0.21
8	576.18±0.02	576.54±0.02	576.02±0.30
9	213.65±0.01	213.15±0.04	211.98±0.18
10	174.86±0.02	174.27±0.03	175.02±0.23
t-test	2.21	2.19	-

Very good correlations between the results obtained using the two stochastic microsensors and ELISA were obtained. Paired t-test was performed at 99.00% confidence level (tabulated theoretical t-value: 4.032) for each microsensor. All calculated t-values were less than the tabulated value, proving that there is no statistically significant difference between the results obtained using the two stochastic microsensors (Table 6.2). Accordingly, the proposed stochastic microsensors can be reliably used for the ultrasensitive determination of 8-OHdG in whole blood samples.

6.4. CONCLUSIONS

The stochastic microsensors based on α -CD/CNT single or multi walled proved to be able to determine the concentration of 8-OHdG in a wide linear concentration range, covering from healthy to patients found on the last stage of breast cancer. The highest sensitivity was recorded for the stochastic sensor based on MWCNT. The feature of the proposed stochastic microsensors is their utilization as screening tools for early diagnosis of breast cancer as well as for determination of the stage of breast cancer. The main advantages are: there are cost-effective tests, no pretreatment of the sample is needed before measurements; the results can be obtained within minutes.

CHAPTER VII

DETERMINATION OF D-SERINE FROM WHOLE BLOOD SAMPLES USING A ZINC (II)-5-(4-CARBOXYPHENYL)-10,15,20-TRIS (4-PHENOXYPHENYL) PORPHYRIN-BASED ELECTROCHEMICAL SENSOR

7.1. INTRODUCTION

In determining the concentration of D-serine in human biological samples, including blood, serum or urine, most researchers rely on HPLC (high-pressure liquid chromatography) [346] and LC-MC (liquid chromatography-mass spectrometry) techniques [347-349].

Some of the properties of porphyrin can be attributed to nanostructured materials based on porphyrin derivatives, namely metallo-derivatives, which have some of the optimal characteristics in electrochemical applications, being used as modifiers.

These metal derivatives include a porphyrin core which has an additional electron conjugation in its structure, and the introduction of a metal ion, results in enhanced electron movement capacity. Of the metal ions, those with the highest electrocatalytic behavior are copper, nickel, iron [366] and cobalt.

Sensors that have been designed using carbon and gold pastes [367] have proven to be important in the detection of clinical [368] and pharmaceutical analytes due to their demonstrated reliability in providing useful analytical information; sensor enhancement with suitable material has amplified the sensor response [368,369-374].

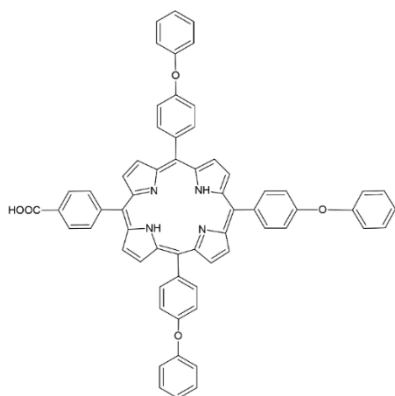


Figure 7.1. The chemical structure of 5-(4-carboxyphenyl)-10,15,20-tris(4-phenoxyphenyl)porphyrin

The utilization of electrochemical sensors for biomedical analysis [353-361] has many advantages: the method is fast and reliable, and the sample does not need any pretreatment [362-364].

The possible mechanism of electrochemical oxidation of D-serine is illustrated in Figure 7.2, with the detection of D-serine via the stoichiometric product of hydrogen peroxide during the D-serine oxidation process. The proposed method was differential pulse voltammetry (DPV). The sensor was validated using whole blood samples.

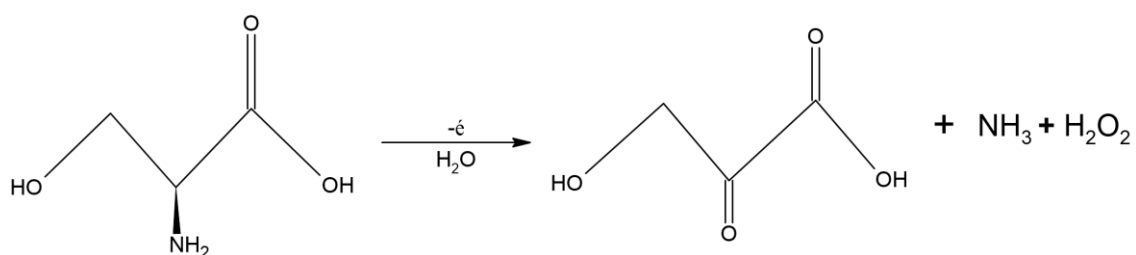


Figure 7.2. The possible mechanism of the electrochemical oxidation of D-serine on the surface of the modified nanographene paste.

7.2. EXPERIMENTAL PART

7.2.1. Materials and reagents

L- and D-serine, D-tryptophan, D-arginine, D-aspartic acid, Zn(II)-5(4-carboxyphenyl)-10,15,20-tris(4-phenoxyphenyl) porphyrin and nanographene. D-Serine solutions were prepared freshly each day in phosphate buffer solution (PBS, pH=7.5).

7.2.2 Apparatus

All experimental measurements were performed using an AUTOLAB/PGSTAT 302 (Metrohm, Utrecht, The Netherlands), connected to a computer for data acquisition. The electrochemical cell consists of three electrodes: a reference electrode (Ag/AgCl, 0.1 mol/L KCl), a working electrode (the proposed electrochemical sensor) and a counter electrode (platinum wire).

7.2.3. Design of the electrochemical sensor

Nanographene powder was mixed with paraffin oil to obtain a homogeneous paste, which was subsequently modified with Zn(II)-5(4-carboxyphenyl)-10,15,20-tris(4-phenoxyphenyl) porphyrin. A plastic tip was filled with modified nanographene paste. The electrical contact was an Ag wire. The sensor surface was washed with modified nanographene

paste. The electrical contact was an Ag wire. The sensor surface was washed with deionized water and polished with paper before each use.

7.2.4. Recommended procedure

DPV measurements were performed at 25⁰C for each standard solution (10⁻³-10⁻¹³mol/L). Peak height intensities were measured and calibration equations were found using the linear regression method. Unknown concentrations were calculated from the statistically determined calibration equation.

The working parameters were as follows: the scan rate was 10 mV s⁻¹ , intervalul de potential range from -0.5 to -0.1V and the modulation amplitude 25 mV.

7.2.5. Samples

Whole blood samples were obtained from the University Emergency Hospital Bucharest (ethics committee approval no. 75/2015) from 3 different patients diagnosed with breast cancer. These samples were used for direct D-serine assay without any pretreatment.

7.2.6. Selectivity studies

The electrochemical sensor selectivity study was performed against: D-trp, D-Glu, D-Srg, L-Ser and D-aspartic acid. To determine the selectivity of the proposed electrochemical sensor, the amperometric selectivity coefficients were determined by the mixed solutions method to determine if there is interference. Solutions were prepared according to the mixed solutions method prior to measurements, taking into account the ratio of 1:10 (mol/mol) between D-serum and interferant. The method was used for a good understanding of the electrode use under efficient conditions and is thus a recommended procedure for determining amperometric selectivity coefficients.

7.3. RESULTS AND DISCUSSIONS

7.3.1. Characteristic response of the proposed electrochemical sensor

DPV was used to determine the response characteristics of the electrochemical sensor. The voltammograms used to calibrate the proposed sensor were shown in Figure 7.3.

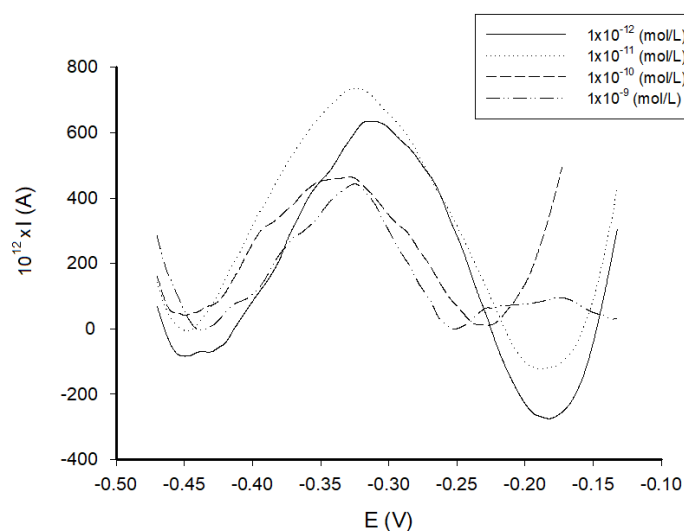


Figure 7.3. Differential pulse voltammogram obtained for D-serine at different concentrations. The working parameters were as following: scan rate was 10 mV s^{-1} , potential range from -0.5 to -0.1 V , and modulation amplitude 25 mV .

The half-wave potential was recorded at $-0,248 \text{ mV}$ for $1 \times 10^{-8} \text{ mol/L}$ D-serine. Figure 7.4. shows the calibration curve. The response characteristics obtained were: the linear concentration range was $1 \times 10^{-12} \text{ mol/L}$ x $1 \times 10^{-9} \text{ mol/L}$, and the limit of determination was $5 \times 10^{-13} \text{ mol/L}$. The equation of calibration was:

(1)

$$I = 3.02 \times 10^{-10} + 0.52 \times C_{D\text{-serine}}$$

where I is the current in A, $C_{D\text{-serine}}$ is the concentration of D-serine in mol/L. The correlation coefficient, r is 0.9949 . The results showed a good value of the sensitivity (0.52 A/mol/L) and a low limit of detection (0.5 pmol/L) for D-serine. The linear concentration range is wide.

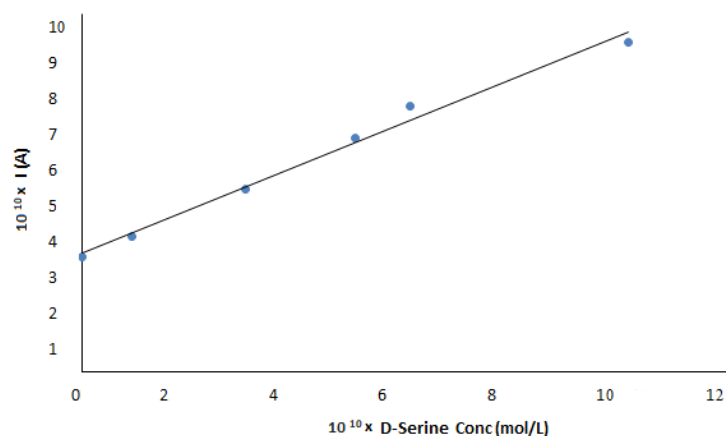


Figure 7.4. Calibration graph obtained for D-serine using the modified nanographene paste based sensor.

The half-wave potential was recorded at -0.248 mV for 1×10^{-8} mol/L D-serine. Figure 7.4 shows the calibration curve. The response characteristics obtained were: the linear concentration range was 1×10^{-12} mol/L x 1×10^{-9} mol/L and the limit of determination was 5×10^{-13} mol/L.

Compared with the stochastic sensor proposed earlier for the assay of D-serine [373], the proposed electrochemical sensor exhibited better sensitivity; also the determination of D-serine with this electrochemical sensor can be performed faster.

7.3.2. Selectivity of the electrochemical sensor

The amperometric selectivity coefficients were determined using the following equation [374]:

$$K_{i,j}(\text{amp}) = \left(\frac{\Delta I_t}{\Delta I_i} - 1 \right) * \frac{c_i}{c_j} \quad (2)$$

where $K_{i,j}(\text{amp})$ is the amperometric selectivity coefficient,,

$$\Delta I_t = \Delta I_i - \Delta I_b,$$

where ΔI_t is the total intensity of the current, ΔI_b is the intensity of the current recorded for blank solution, $\Delta I_i = \Delta I_t - \Delta I_b$, where ΔI_i is the intensity of the current registered for main ion, c_i and c_j are the concentrations of the main ion and the interfering ions.

Mixed solution method was used for the determination of potential interferences in the assay of D-ser. The values obtained for the coefficients are shown in Table 7.1.

Table 7.1. Amperometric selectivity coefficients

Parameters	Analyte	Interferent (10 ⁻³ M)	K_{sel}^{amp}
scan rate 10 mV s ⁻¹	D- Serine (10 ⁻⁴ M)	D-Trp	1.05x10 ⁻⁴
		D-Glu	2.09x10 ⁻³
D-Arg		1.45x10 ⁻³	
L-Ser		1.14x10 ⁻³	
D-Asp Acid		7.37x10 ⁻⁴	
potential range -0.5 ÷ 0.1 V			
modulation amplitude 25 mV			

Amperometric coefficients were determined using the same potential that was used for the determination of D-serine using the proposed sensor. The results show that there is no interference of D-Trp and D-Asp acid and low interference of D-Glu, D-Arg and L-ser in the determination of D-serine.

7.3.3. Determination of D-serine in whole blood samples

DPV was used for the determination of D-serine in three whole blood samples. The electrochemical cell containing the three electrodes was immersed in the cell which was filled With blood samples. The results of the measurements are shown in Table 7.2. An example of the voltammogram obtained for the whole blood sample is shown in Figure 7.5. which is an inset enlargement for better understanding. To perform the recovery test, the following mechanism was adopted: D-serine were added. The recovered amounts were compared with those that were inserted into the biological samples. A classical method was used to determine D-serine from the biological sample. The results obtained using DPV correlated well with the result obtained by HPLC, but in general, better results were obtained using electrochemistry (Table 7.2.).

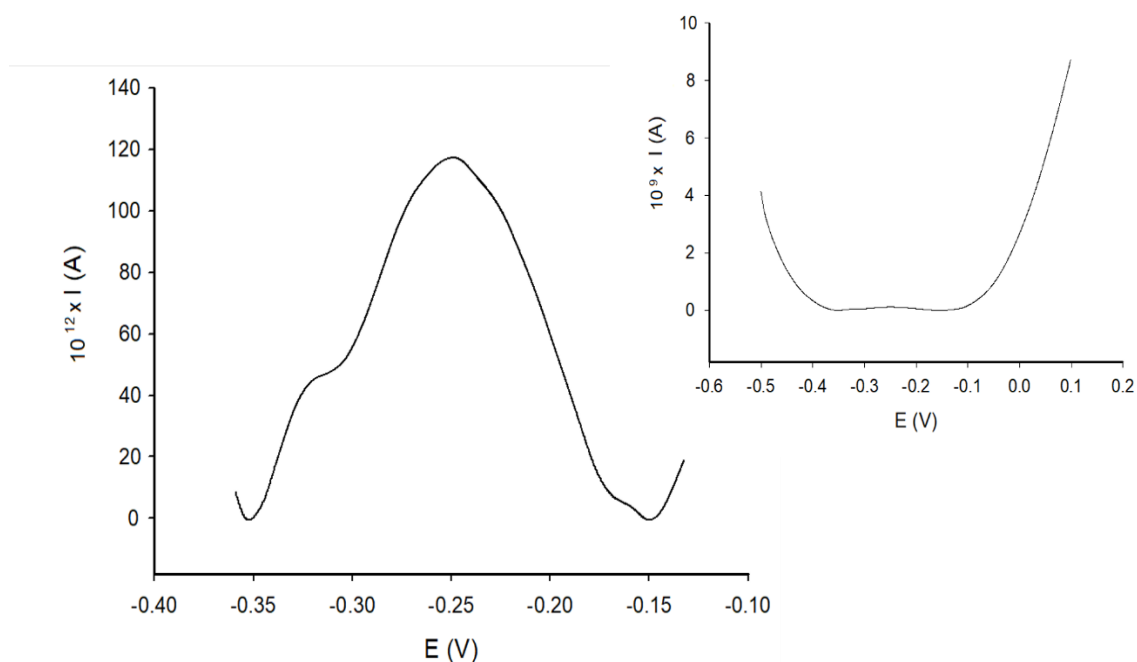


Figure 7.5. Example of voltammogram obtained for the assay of D-serine in whole blood sample. The working parameters were as following: scan rate was 10 mV s^{-1} , potential range $-0.5 \div 0.1 \text{ V}$, and modulation amplitude 25 mV.

Table 7.2. Determination of D-serine in whole blood samples using the proposed electrochemical sensor (scan rate was 10 mV s^{-1} , potential range $-0.5 \div 0.1 \text{ V}$, and modulation amplitude 25 mV) and HPLC data

Sample No.	$\mu\text{mol L}^{-1}$, D-serine	
	DPV Electroanalysis*	HPLC [11]
1	2.57 ± 0.12	2.50 ± 1.14
2	2.86 ± 0.13	2.70 ± 1.20
3	3.80 ± 0.12	3.20 ± 1.40

* Using the proposed electrochemical sensor

7.4. CONCLUSIONS

An electrochemical sensor based on physical immobilization of Zn(II)-5(4-carboxyphenyl)-10,15,20-tris(4 phenoxyphenyl)porphyrine has been proposed for the analysis of D-Serine in whole blood samples. The electrochemical sensor showed high selectivity, as well as low limits of detection and determination, and high sensitivity. The sensor was validated using whole blood samples.

GENERAL CONCLUSIONS AND FUTURE PERSPECTIVES

GENERAL CONCLUSIONS

Over the years there has been an evolution in the progression of biomedical, pharmaceutical, chemical and physical analysis methods with the aim of developing some innovative, state-of-the-art methods to improve cancer detection and screening prevention.

Tumor markers (CA15-3, CEA, HER-1, HER-2, heregulin- α , 8-OHdG) studied in the PhD thesis have an important role in the early detection and diagnosis of certain diseases by preventing, curing or halting their progression.

The aim of the PhD thesis was to develop methods for the determination of compounds of Biomedical interest based on stochastic sensor design. The experimental part included the development, construction and validation of stochastic sensors based on functional materials (copper, zinc, graphene, diamond), modified with certain electroactive materials (carbon nanopowder, pentafluorophenyl chloride, porphyrin). In the analysis and validation of stochastic methods were used biological samples (blood) obtained in collaboration with the University Hospital of Bucharest.

The determination of D-serine and D-leucine has been a key factor in the development and use of enantioselective stochastic for screening of biological samples (blood-whole blood samples).

Enantioselective analysis of whole blood samples obtained from both confirmed breast cancer patients and healthy volunteers detected only the presence of the D-serine enantiomer in cancer patients, not in healthy volunteers.

The values obtained using the sensor showed a good correlation between the results obtained by the stochastic method and ELISA. This method demonstrated that D-serine can be a biomarker for early diagnosis of breast cancer.

Biomarker testing was determined simultaneously using three stochastic nC-based microsensors modified with gold nanoparticles and two porphyrins (tetraphenyl, tetrakis) in simultaneous assay of CEA, CA15-3 and HER-2, as a screening test based on their simultaneous analysis will provide more information about personalized breast cancer diagnosis and treatment.

For the ultrasensitive determination of the three biomarkers, HER-1, HER-2 and heregulin- α , two stochastic microsensors based on spheroidal copper-decorated nanographene

and modified with N-(pyridine-3-yl-methyl) oleamide and N-(2-mercapto-1H-benzo[d]imidazole-5-yl) oleamide were successfully used in whole blood samples. A key feature of these sensors is their use as new tools in screening tests of blood samples and tumor tissue. A wide concentration range was obtained by analysing HER-1 using the O₁-based microsensor, for the analysis of HER-2, an identical working concentration range was obtained for both sensors, while a wider concentration range was obtained for the O₂-based microsensor when analysing heregulin- α .

Determination of 8-OHdG concentration in a linear range encompassing both healthy individuals and late-stage breast cancer volunteers has been demonstrated using single- and multi-walled α -CD/CNT-based microsensor showed lower sensitivity. The MWCNT-based stochastic sensor showed the highest sensitivity recorded for the determination of 8-OHdG, whereas the use of the SWCNT-based microsensor showed lower sensitivity. The proposed stochastic microsensors are characterized by their use as screening tools for early breast cancer diagnosis. Some of the main advantages of the sensors are their cost-effectiveness, the fact no pre-treatment of the sample is required before measurement, thus obtaining a result within minutes.

In the molecular recognition of D-serine using electrochemical sensor based on physical immobilization of Zn(II)-5(4-carboxyphenyl)-10,15,20-tris(4-phenophenyl) porphyrin, it showed high selectivity and sensitivity as well as low detection limit for the determination of D-serine from biological samples. The newly presented technique, DPV, was used to determine the response characteristics of the electrochemical sensor. The proposed new methods can be used for rapid screening tests in blood samples for breast cancer diagnosis.

ORIGINAL CONTRIBUTIONS

The fundamental aim of the PhD thesis was: the development of innovative methods in diagnostics using stochastic (electrochemical) sensors based on functional materials: copper, zinc, graphene, diamond, as well as the use of the following electroactive materials: carbon nanopowder, pentafluorophenyl chloride, porphyrin, N-pyridin-3-yl-methyl) oleamide and N-2-mercapto-1H-benzo[d]imidazole-5-yl) oleamide. Detection of different substances of biomedical interest (CA15-3, CEA, HER-1, HER-2, Heregulin- α , 8-OHdG) was performed using stochastic analysis to identify breast cancer specific biomarkers from biological samples. Of particular importance was the identification of D-serine and D-leucine as possible biomarkers in the early diagnosis of breast cancer.

PROSPECTS FOR FURTHER DEVELOPMENT

In the observation and further analysis of new biomarkers or a panel of biomarkers, innovative screening methods based on electrochemical sensors can be proposed, which can use functional and electroactive materials leading to rapid, concise and accurate analysis and response in the precise diagnosis of certain diseases in tumor tissues. Through early diagnosis of various diseases using screening of the population with or without risk factors, detection of tumour markers using stochastic sensors can be used by introducing personalized treatment.

As a future perspective, it is aimed to validate stochastic sensors by implementing them in medical units, clinical laboratories and individual practices for use as rapid screening methods.

ANNEX 1

LIST OF PAPERS PRESENTED AT CONFERENCES

POSTER AND ORAL PRESENTATION

1. CARBON NANOPOWDER BASED STOCHASTIC SENSOR FOR ULTRASENSITIVE ASSAY OF CA 15-3, CEA AND HER2 IN WHOLE BLOOD authored by: *Oana-Raluca Muşat, Raluca-Ioana Ştefan-van Staden, Damaris-Cristina Gheorghe, Ruxandra-Maria Ilie-Mihai, Jacobus Frederick van Staden*, presented at the XVIII th International Symposium PRIOCHEM “Priorities of Chemistry for a Sustainable Development” October 26-28, 2022.

ANNEX 2

PUBLISHED ARTICLES:

1. **Oana-Raluca Musat** & Raluca-Ioana Stefan-van Staden (2022) Stochastic Sensors for the Enantioselective Determination of Serine in Blood for the Early Diagnosis of Breast Cancer, *Analytical Letters*, 55:13, 2124-2131, DOI: 10.1080/00032719.2022.2047999, **F.I.=2.267**.

2. Stefan-van Staden R.-I., **Musat Oana-Raluca**; Gheorghe, D.-C.; Ilie-Mihai, R.-M.; van Staden, J. (Koos) F. Carbon Nanopowder-Based Stochastic Sensor for Ultrasensitive Assay of CA 15-3, CEA and HER2 in Whole Blood. *Nanomaterials* 2022, 12, 3111. <https://doi.org/10.3390/nano12183111>, **F.I.=5.719**.

3. Raluca-Ioana Stefan-van Staden, **Oana-Raluca Musat**, Damaris-Cristina Gheorghe, Ruxandra-Maria Ilie-Mihai a,*, Catalina Cioates Negut, Paula Sfirloaga, Ultrasensitive assay of HER1, HER2, and heregulin- α in whole blood, *Talanta Open* 6 (2022) 100151, received 6 June 2022; Received in revised form 7 September 2022; Accepted 14 September 2022, <https://doi.org/10.1016/j.talo.2022.100151>, S.I.= 1.9.

4. **Oana-Raluca Musat**, Ruxandra-Maria ILIE-MIHAI, Raluca-Ioana STEFAN-VAN STADEN, Determination of d-serine from whole blood samples using an electrochemical sensor based on zinc (ii) – 5(4-carboxyphenyl)-10,15,20- tris(4 phenoxyphenyl)porphyrine , *U.P.B. Sci. Bull.*, Series B, Vol. 84, Iss. 4, 2022 ISSN 1454-2331.

F.I. cumulativ: 7.986

ARTICLES SUBMITTED FOR PUBLICATION:

1. Ultrasensitive assay of 8-hydroxy-2'-deoxyguanosine in whole blood using carbon nanotubes based stochastic microsensors, *Electrochem Comm*, Raluca-Ioana Stefan-van Staden, Oana-Raluca Musat.

2. Enantioanalysis of leucine in whole blood samples using enantioselective, stochastic sensors, *Chemosensors* Raluca-Ioana Stefan-van Staden, Oana-Raluca Musat.

SELECTED REFERENCES

- [1]. *Ferlay J, Soerjomataram I, Ervik M, Dikshit R, Eser S, Mathers C, Rebelo M, Parkin DM, Forman D, Bray F. GLOBOCAN 2012 v1.0, Cancer Incidence and Mortality Worldwide: IARC CancerBase No. 11 [Internet]. Lyon, France: Intl Agency for Research on Cancer, 2013, Available from.<http://globocan.iarc.fr>.*
- [2]. *Bray F, Ren JS, Masuyer E, Ferlay J (2013). Global estimates of cancer prevalence for 27 sites in the adult population in 2008. Int J Cancer, 132(5):1133–45 <http://dx.doi.org/10.1002/ijc.27711> PMID:22752881.*
- [3]. *Althuis MD, Fergenbaum JH, Garcia-Closas M, Brinton LA, Madigan. Etiology of hormone receptor-defined breast cancer: a systematic review of the literature. Cancer Epidemiology Biomarkers and Prevention, 2004, 13(10):1558-68.*
- [4]. *Piccart-Gebhart M.J. New developments in hormone receptor-positive disease. The oncologist., 2011, 16:40-50.*
- [5]. *Leal M. F., Assumpção P. P., Smith M. C., Burbano R. R., Searching for Gastric Cancer Biomarkers Through Proteomic Approaches, J. Gastroenterol. Hepatol., vol.3, no.3, 2014, 989-995.*
- [6]. *Pankaj Taneja, Dejan Maglic, Fumitake Kai, Sinan Zhu, Robert D. Kendig Classical and Novel Prognostic Markers for Breast Cancer and their Clinical Significance. Clin Med Insights Oncol, 2010,4:15-34.*
- [7]. *Fisher B, Constantino JP, Wickerham DL. Tamoxifen for prevention of breast cancer report of the National Surgical Adjuvant Breast and Bowel Project P-1 Study. J Natl Cancer Inst, 1998, 90(18):1371-88.*
- [8]. *Slamon DJ, Clark GM et al. Human breast cancer correlation of relapse and survival with amplification of HER-2/neu oncogene. Science, 1987, 235(4785):177-82.*
- [9]. *Stuart-Harris R, Caldas C, Pinder SE, Pharoah P. Proliferation markers and survival in early breast cancer: a systematic review and meta-analysis of 85 studies in 32,825 patients. Breast, 2008, 17(4):323–334.*
- [10]. *Assersohn L, Salter J, Powles TJ, A'Hern R, Makris A, Gregory RK, Chang J, Dowsett M. Studies of the potential utility of Ki67 as a predictive molecular marker of clinical response in primary breast cancer. Breast Cancer Res Treat, 2003, 82:113-23.*

- [11]. *Jones RL, Salter JA*. The prognostic significance of Ki67 before and after neoadjuvant chemotherapy in breast cancer *Clin Cancer Res*, **2008**, 14:8019-26.
- [12]. *Uehara M, Kinoshita T, Hojo T, Akashi-Tanaka, Iwamoto E*. Long-term prognostic study of carcinoembryonic antigen (CEA) and carbohydrate antigen 15-3 (CA 15-3) in breast cancer. *Int J Clin Oncol*, **2008**, 13(5):447-51.
- [46]. *Fleissig A, Jenkins V, Catt S, Fallowfield L*. Multidisciplinary teams in cancer care: are they effective in the UK? *Lancet Oncol*, **2006**, 7:935-43.
- [65]. *Petrucelli N, Daly BM, Feldman LG*, BRCA1 and BRCA2 Hereditary Breast and Ovarian Cancer. *Gene Reviews*, **2007**, www.ncbi.nlm.nih.gov.
- [66]. *Welesh PL, King MC*. BRCA1 and BRCA2 and the genetics of breast and ovarian cancer, *Hum Mol Genet*, **2001**, 10(7):705-13.
- [67]. *Uehara M, Kinoshita T, Hojo T, Akashi-Tanaka, Iwamoto E*. Long-term prognostic study of carcinoembryonic antigen (CEA) and carbohydrate antigen 15-3 (CA 15-3) in breast cancer. *Int J Clin Oncol*, **2008**, 13(5):447-51.
- [71]. *Pasaoglu G, Zamani A, Can G, Imecik O*. Diagnostic value of CEA, CA-19-9, CA 125 and CA 15-3 levels in malignant pleural fluids. *Eur J Gen Med.*, **2007**, 4(4):165–71.
- [72]. *Yamagata K, Izawa Y, Onodera D, Tagami M*, **2018**, Chlorogenic acid regulates apoptosis and stem cell marker-related gene expression in A549 human lung cancer cells. *Molecular and cellular biochemistry* 441(1-2):9-19.
- [75]. *Dr.Liz O’Riordan Professor Trisha Greenhalgh* – The Complete Guide to Breast Cancer. How to Feel Empowered and Take Control.
- [87]. *Jones RL, Salter JA*. The prognostic significance of Ki67 before and after neoadjuvant chemotherapy in breast cancer *Clin Cancer Res*, **2008**, 14:8019-26.
- [88]. *Mastropasqua MG, Viale G*, **2017**, Clinical and pathological assessment of high-risk ductal and lobular breast lesions: What surgeons must know. *European journal of surgical oncology: the journal of the European Society of Surgical Oncology and the British Association of Surgical Oncology* 43(2):278-284.
- [89]. *Jager W, Eibner K, Loffler B, Gleixner S*, et al. Serial CEA and CA 15-3 measurement during follow-up of breast cancer patients *Anticancer Res*, **2000**, 20(6):5179-28.

- [100]. Jo, Y.; Lee, J.H.; Cho, E.S.; Lee, H.S.; Shin, S.J.; Park, E.J.; Baik, S.H.; Lee, K.Y.; Kang, J. Clinical significance of early carcinoembryonic antigen change in patients with nonmetastatic colorectal cancer. *Front.Oncol.*, **2022**, *12*, 739614.
- [101]. Goossens N., Nakagawa S., Sun X., Hoshida Y. Cancer biomarker discovery and validation, *Translational Cancer Research*, **2015**, *4*, 256–269.
- [107]. Blakeman V, Williams JL, Meng QJ, Streuli CH. Circadian clocks and breast cancer. *Breast Cancer Res.*,**2016**.Sep 2,18(1):89.
- [108]. Kollias J, Ellis IO, Elston CW, Blamey RW - Clinical and histological predictors of contralateral breast cancer. *Eur JSurg Oncol*,**1999**,*25*, 584-589.
- [112]. Siegel RL, Miller KD, Jemal A. Cancer statistics, 2019. *CA Cancer J Clin*, **2019**, Jan;69(1):7-34.
- [117]. Kroman N, Holtveg H, Wohlfahrt J, Jensen M-B, Mouridsen HT, Blichert-Toft M, et al. Effect of breastconserving therapy versus radical mastectomy on prognosis for young women with breast carcinoma. *Cancer*, **2004**;100: 68893.
- [126]. McGale P, Taylor C, Correa C, et al. EBCTCG (Early Breast Cancer Trialists' Collaborative Group) Effect of radiotherapy after mastectomy and axillary surgery on 10-year recurrence and 20-year breast cancer mortality: Meta-analysis of individual patient data for 8135 women in 22 randomised trials. *Lancet.*, **2014**;383:2127–2135.
- [131]. Braik T., Gupta S., Poola H., Jain P., Beiranvand A., Lad T.E., Hussein L. Carcino embryonic antigen (CEA) elevation as a predictor of better response to first line pemetrexed in advanced lung adenocarcinoma. *J. Thorac. Oncol.*, **2012**, *7*, S310.
- [132]. Staden R (11 d.Hr.). „A strategy of DNA sequencing employing computer programs”. *Nucleic Acids Research*. 6 (7): 2601–10. doi:10.1093/nar/6.7.2601. PMC 327874 . PMID 461197.
- [133]. de Magalhães JP, Finch CE, Janssens G, **2010**, „Next-generation sequencing in aging research: emerging applications, problems, pitfalls and possible solutions”. *Ageing Research Reviews*. 9 (3): 315–323. doi:10.1016/j.arr.2009.10.006. PMC 2878865. PMID 19900591.
- [134].^ Hall N , mai **2007**, „Advanced sequencing technologies and their wider impact in microbiology”. *J. Exp. Biol*. 209 (Pt 9): 1518-1525. doi:10.1242/jeb.001370. PMID 17449817.

- [135].[^] *Church GM*, ianuarie **2006**, „Genomes for all”. *Sci. Am.* *294 (1): 46–54*. doi:10.1038/scientificamerican0106-46. PMID 16468433.
- [136]. [^] *Quail MA, Smith M, Coupland P, Otto TD, Harris SR, Connor TR, Bertoni A, Swerdlow HP, Gu Y*, 1 ianuarie **2012**, „A tale of three next generation sequencing platforms: comparison of Ion Torrent, Pacific Biosciences and illumina MiSeq sequencers”. *BMC Genomics.* *13(1):341*. doi:10.1186/1471-2164-13-341. PMC 3431227. PMID 22827831.
- [165]. *Huang YF, Chen SC, Chiang YS, Chen TH, Chiu KP*, **2012**, „Palindromic sequence impedes sequencing-by-ligation mechanism”. *BMC Systems Biology.* *6 Suppl 2: S10*. doi:10.1186/1752-0509-6-S2-S10. PMID 23281822.
- [179]. *Greenblatt, M.S., Bennett, W.P., Hollstein, M., and Harris, C. C.* Mutations in the p53 tumor suppressor gene: clues to cancer etiology and molecular pathogenesis. *Cancer Research*, **1994**, *54*, 4855–4878.
- [180]. *Be´roud, C., and Soussi, T.* p53 gene mutation: software and database. *Nucleic Acids Research*, **1998**, *26*, 200–204.
- [181]. *Gold P., Freedman S.O.* Demonstration of tumour specific antigens in human colon carcinomata by immunological tolerance and absorption techniques. *Journal of Experimental Medicine*, **1965**, *121*, 439-62.
- [185]. *Ribeiro-Silva A, Zamzelli Ramalho LN, Garcia SB*, et al. - Is p63 reliable indetecting microinvasion in ductal carcinoma in situ of the breast? *Pathol Oncol Res*, **2003**, *9:20–3*.
- [210]. *Lyon, D.H., Francombe, M.A., Hasdell, D.A. & Lawson, K.*, **1992**, Guidelines for Sensory Analysis in Food Product Development and Quality Control.
- [211]. *Muñoz, A.M., Civille, G.V. & Carr, B.T.*, **1992**, Sensory Evaluation in Quality Control.
- [213]. *De Vos, E.* (2010) Selection and management of staff for sensory quality control. In Kilcast, D. (Eds.) *Sensory Analysis for Food and Beverage Quality Control* (pp. 17-36).
- [214]. ”Stochastic Methods in Neuroscience”, *C. Laing, G.J. Lord*, Oxford University Press, New York, **2010**.

- [217]. *Q Zhao, DA Jayawardhana, X Guan, Biophys J* 94, 1267-1275, **2008**.
- [221]. 21. A Aksimentiev, *JB Heng, G Timp, K. Schulten, Biophys J* 87, 2086-2097, **2004**.
- [229]. *Stefan-van Staden R. I., Popa-Tudor I., Ionescu-Tirgoviste C., Stoica R. A.*, Molecular recognition of pyruvic acid and L-lactate in early-diabetic stage, *J. Electrochem. Soc.*, vol.165, **2018**, B659-B664.
- [230]. *Gugoasa L. A., Stefan-van Staden R. I., Dima A., Visan C. A., Streinu-Cercel A., Biris A., Calenic B.*, Fast screening of biological fluids for cytokines and adipokines using stochastic sensing, *Microelectron. Eng.*, vol.148, **2015**, 64-69.
- [231]. *Ates B, Koytepe S., Ulu A., Gurses C., Thakur V. K.*, Chemistry, structures, and advanced applications of nanocomposites from biorenewable resources, *Chem. Rev.*, **2020**.
- [232]. *Wróblewska-Krepsztul J., Rydzkowski T., Michalska-Požoga I.; Thakur V. K.*, Biopolymers for biomedical and pharmaceutical applications: recent advances and overview of alginate electrospinning, *Nanomaterials*, vol.9, **2019**, 404.
- [233]. *Siwal S. S., Zhang Q., Sun C., Thakur V. K.*, Graphitic carbon nitride doped copper–manganese alloy as high–performance electrode material in supercapacitor for energy storage, *Nanomaterials*, vol.10, , no.1, **2020**, 2.
- [327]. *A. Valavanidis, T. Vlachogianni, C. Fiotakis*, 8-hydroxy-2'-deoxyguanosine (8-OHdG). A critical biomarker of oxidative stress and carcinogenesis, *J. Environ. Sci. Health C. Environ. Carcinog. Ecotoxicol. Rev.* 27, **2009**, 120-139, <https://doi.org/10.1080/10590500902885684>.
- [328]. *E.E.M.N. Eldin, M.Z. El-Readi, M.M.N. Eldein, A.A. Alfalki, M.A. Althubiti, A.A. Mirza*, 8-hydroxy-2'-deoxyguanosine as a discriminatory biomarker for early detection of breast cancer, *Clin. Breast Cancer* 19, **2019**, e385-e393, <https://doi.org/10.1016/j.clbc.2018.12.013>.
- [329]. *J. Musarrat, J. Arezina-Wilson, A.A. Wani*, Prognostic and aetiological relevance of 8-hydroxyguanosine in human breast carcinogenesis, *Eur. J. Cancer* 32A, **1996**, 1209-1214, [https://doi.org/10.1016/0959-8049\(96\)00031-7](https://doi.org/10.1016/0959-8049(96)00031-7).
- [330]. *K. Shimol, H. Kasai, N. Yokota, S. Toyokuni, N. Kinoshita*, Comparison between high-performance liquid chromatography and enzyme-linked immunosorbent assay for the

- determination of 8-hydroxy-2'-deoxyguanosine in human urine, *Cancer Epidemiol.Biomarkers Prev.* 11, **2002**, 767-770.
- [331]. *D. Germadnik, A. Pilger, H.W. Rüdiger*, Assay for the determination of urinary 8-hydroxy-2'-deoxyguanosine by high performance liquid chromatography with electrochemical detection, *J. Chromatogr. B* 689, **1997**,399-403, [https://doi.org/10.1016/S0378-4347\(96\)00328-3](https://doi.org/10.1016/S0378-4347(96)00328-3).
- [332]. *J. Xu, J. Zhang, R. Zeng, L. Li, M. Li, D. Tang*, Target-induced photocurrent-polarity-switching photoelectrochemical aptasensor with gold nanoparticle-ZnIn₂S₄ nanohybrids for the quantification of 8-hydroxy-2'-deoxyguanosine, *Sens.Actuators B* 368, **2022**, 132141, <https://doi.org/10.1016/j.snb.2022.132141>.
- [333] *.J. Thangphatthanarungruang, C. Chotsuwan, S. Jampasa, W. Siangproh*, A new nanocomposite-based screen-printed graphene electrode for sensitive and selective detection of 8-hydroxy-2'-deoxyguanosine, *FlatChem* 32, **2022**, 100335, <https://doi.org/10.1016/j.flatc.2022.100335>.
- [346]. *T. Fukushima, J. Kawai, K. Imai, T. Toyo'oka*, “Simultaneous determination of D- and L-Serine in rat brain microdialysis sample using a column-switching HPLC with fluorimetric detection”, *Biomedical Chromatography*, vol.18, **2004**, pp. 813-819.
- [347]. *E.A.L.M. Biemans, N.M. Verhoeven-Duif, J. Gerrits, J.A.H.R. Claassen, H.B. Kuiperij, M. M. Verbeek*, “CSF D-Serine concentrations are similar in Alzheimer's disease, other dementias, and elderly controls”, *Neurobiology of Aging*, vol.42, **2016**, pp. 213-216.
- [348] *S.L. Grant, Y. Shulman, P. Tibbo, D.R. Hampson, G.B. Baker*, “Determination of D-Serine and related neuroactive amino acids in human plasma by high-performance liquid chromatography with fluorimetric detection”, *Journal of Chromatography B: Analytical Technologies in the Biomedical and Life Sciences*, vol.844, **2006**, pp. 278-282.
- [349]. *D. Koval, J. Jirásková, K. Stríšovský, J. Konvalinka, V. Kašička*, “Capillary electrophoresis method for determination Of D-Serine and its application for monitoring of serine racemase activity”, *Electrophoresis*, vol.27, **2006**, pp. 2558-2566.

- [366]. *D. Vlascici, E. Fagadar-Cosma, I. Popa, V. Chiriac, M. Gil-Agusti*, “A novel sensor for monitoring of iron(III) ions based on porphyrins”, *Sensors (Basel)*, vol.12, **2012**, pp. 8193-8203.
- [367]. *C. Epuran, I. Fratilescu, A.M. Macsim, A. Lascu, C. Ianasi, M. Birdeanu, E. Fagadar-Cosma*, “Excellent cooperation between carboxyl-substituted porphyrins, k-carrageenan and AuNPs for extended application in CO₂ capture and manganese ion detection”, *Chemosensors*, vol.10, **2022**, 133. DOI: 10.3390/chemosensors10040133.
- [368]. *L. Sălăgeanu, D. Muntean, M. Licker, A. Lascu, D. Anghel, E. Fagadar-Cosma*, “Symmetrical and asymmetrical meso-substituted porphyrins and zn-metalloporphyrins in gold colloid environment. optical properties and evaluation of antibacterial activity”, *Farmacia*, vol.68, **2020**, pp. 288-298.
- [369]. *E. Fagadar-Cosma, D. Vlascici, M. Birdeanu, G. Fagadar-Cosma*, “Novel fluorescent pH sensor based on 5-(4-carboxy-phenyl)-10,15,20-tris(phenyl)-porphyrin”, *Arabian Journal of Chemistry*, vol.12, **2019**, pp. 1587-1594.
- [370]. *A.M. Iordache, R. Cristescu, E. Fagadar-Cosma, A.C.Popescu, A.A. Ciucu, S.M. Iordache, A. Balan, C. Nichita, I. Stamatin, D.B. Chrisey*, “Histamine detection using functionalized porphyrin as electrochemical mediator”, *Comptes Rendus Chimie*, vol.21, **2018**, pp. 270-276.
- [371]. *K. Nemčėková, J. Labuda*, “Advanced materials-integrated electrochemical sensors as promising medical diagnostics tools: A review”, *Materials Science and Engineering C*, vol.120, **2021**, 111751. DOI: 10.1016/j.msec.2020.111751.
- [372]. *R.I. Stefan-van Staden, D.C. Gheorghe, V. Jinga, C.S. Sima, M. Geanta*, “Fast screening of whole blood and tumor tissue for bladder cancer biomarkers using stochastic needle sensors”, *Sensors*, vol.20, **2020**, 2420. DOI: 10.3390/s20082420.
- [373]. *O.R. Musat, R.I. Stefan-van Staden*, “Stochastic sensors for the enantioselective determination of serine in blood for the early diagnosis of breast cancer”, *Analytical Letters.*, vol.55, no. 13, **2022**, pp. 2124-2131.
- [374]. *R.I. Stefan, J.F. van Staden, H.Y. Aboul-Enein*, “Electrochemical sensors in Bioanalysis”, Taylor & Francisc, Routledge, USA, **2001**.
- [354]. *J.G. Pacheco, S.V. Marta, S.M. Freitas, H.P.A. Nouws, C. Delerue-Matos*, “Molecularly imprinted electrochemical sensor for the point-of-care detection of a

- breast cancer biomarker (CA 15-3)”, *Sensors and Actuators B: Chemical*, vol.256, **2018**, pp. 905-912.
- [355]. *J.G. Pacheco, P. Rebelo, M. Freitas, H.P.A.Nouws, C. Delerue-Matos*, “Breast cancer biomarker (HER2-ECD) detection using a molecularly imprinted electrochemical sensor”, *Sensors and Actuators B: Chemical*, vol.273, **2018**, pp. 1008-1014.
- [356]. *L. Jing, C. Xie, Q. Li, M. Yang, S. Li, H. Li, F. Xia*, “Electrochemical Biosensors for the analysis of breast cancer biomarkers: from design to application”, *Analytical Chemistry*, vol.94, **2022**, pp. 269-296.
- [357]. *B. Mohan, S. Kumar, H. Xi, S.M. Z. Tao, T. Xing, H. You, Y. Zhang, P. Ren*, “Fabricated metal-organic frameworks (MOFs) as luminescent and electrochemical biosensors for cancer biomarkers detection”, *Biosensors and Bioelectronics*, vol.197, **2022**, 113738. DOI: 10.1016/j.bios.2021.113738.
- [358]. *V. Vongsouthi, J.H. Whitfield, P. Unichenko, J.A. Mitchell, B. Breithausen, O. Khersonsky, L. Kremers, H. Janovjak, H. Monai, H. Hirase, S.J. Fleishman, C. Henneberger, C.J. Jackson*, “A rationally and computationally designed fluorescent biosensor for d-serine”, *ACS Sensors*, vol.6, **2021**, pp. 4193-4205.
- [359]. *S. Moussa, M.R. Van Horn, A. Shah, L. Pollegioni, C.J. Thibodeaux, E.S. Ruthazer, J. Mauzeroll*, “A miniaturized enzymatic biosensor for detection of sensory-evoked d-serine release in the brain”, *Journal of the Electrochemical Society*, vol.168, **2021**, 025502. DOI:10.1149/1945-7111/abe348.
- [360]. *C. Cioates Negut, R.I. Stefan - van Staden, J.F. van Staden*, “Porphyrins-as active materials in the design of sensors. an overview”, *ECS Journal of Solid State Science and Technology*, vol.9, **2020**, 051005. DOI:10.1149/2162-8777/ab9a5d.
- [361]. *R.I. Stefan-van Staden, J.F. van Staden*, “Dot microsensors based on zinc porphyrins and zinc phthalocyanine for the determination of indigo carmine”, *ECS Journal of Solid State Science and Technology*, vol.9, **2020**, 041015. DOI:10.1149/2162-8777/ab902e.
- [362]. *M. Coros, S. Pruneanu, R.I. Stefan-van Staden*, “Recent progress in the graphene-based electrochemical sensors and biosensors”, *Journal of the Electrochemical Society*, vol.167, **2020**, 037528. DOI:10.1149/2.0282003JES.

- [363]. *R.I. Stefan-van Staden, I. Moldoveanu, C.S. Gavan*, “Pattern recognition of HER-1 in biological fluids using stochastic sensing”, *Journal of Enzyme Inhibition and Medicinal Chemistry*, vol.30, **2015**, pp. 283-285.
- [364]. *R.I. Stefan-van Staden, I.R. Comnea-Stancu, C.C. Surdu-Bob*, “Molecular screening of blood samples for the simultaneous detection of CEA, HER-1, NSE, CYFRA 21-1 using stochastic sensors”, *Journal of the Electrochemical Society*, vol.164, **2017**, B267. DOI:10.1149/2.1621706jes.

SITE-URI INTERNET

- [2].<http://www.esciencecentral.org/ebooks/cancer-treatment-strategies/cancer-targeting-strategies-revisited.php>